DOE/ER/40481--T1

Low Energy Solar Neutrino Measurements:

The Soviet American Gallium Experiment (SAGE)

Contract No. DE-FG05-88ER40481

Final Report

submitted to

Department of Energy
Office of Energy Research
(Nuclear Physics)

I. Introduction

Direct measurements of the Sun's interior can be obtained either from seismic observations of solar oscillations or from studies of the neutrinos produced by nuclear fusion reactions in the Sun's core. For over twenty years now, the radiochemical ^{37}Cl solar neutrino experiment in the Homestake Gold Mine[1,2] has been monitoring the flux of the relatively high energy neutrinos (mainly from ^{8}B decays in the Sun) with the count rate consistently a factor of 2.5 - 3.5 below the value expected from standard models of solar physics.[3,4] Apparently, either our models of the Sun's interior are incomplete or our understanding of neutrino physics is deficient. Calculated values for the Homestake chlorine experiment are in the range 6-8 SNU (1 solar neutrino unit = 10^{-36} captures/target atom/second), while the measured $\nu_e + {}^{37}Cl \rightarrow {}^{37}Ar + e^-$ production rate is 2.28 ± 0.23 SNU (0.429 ± 0.043 captures/day) after subtracting a terrestrial background of 0.43 ± 0.28 SNU. The low flux at Homestake has been confirmed by Kamiokande,[5] with a rate for events *coming from the direction of the Sun* corresponding to 0.50 ± 0.04 (*stat*) $\pm$ 0.06 (*syst*) times that of Bahcall and Pinnseneault's standard solar model.[3]

The flux of the high energy ^{8}B neutrinos (to which the chlorine and water experiments are most sensitive) is critically dependent on the temperature of the Sun's core. In order to calculate the ^{37}Ar capture rate to within a factor of 3, the solar core temperature must be known to an accuracy of $\delta T/T \sim 10 - 20\%$. Numerous non-standard solar models[6] have therefore been suggested, incorporating a variety of heavy metal abundances, high magnetic fields, turbulent diffusion, continuous mixing, rapidly rotating or burned-out helium cores, convective mixing of hydrogen into the core, or new equations of state. All of these effects go in the direction of lowering the solar core temperature. However, these non-standard models generally have difficulties accounting for other observed features on the Sun.

In addition to solar model effects, it has also been suggested that our understanding of the relevant particle physics may be incomplete. Mikheyev and Smirnov[7] and Wolfenstein[8] have pointed out that the different coupling of ν_e, ν_μ, and ν_τ to matter can cause an oscillation effect: if ν_e and $\nu_{\mu,\tau}$ are linear combinations of the same mass eigenstates, the ν_e produced by ^{8}B decays in the Sun's core can oscillate into ν_μ or ν_τ as they propagate outward through the sun's overlying layers. The chlorine detector is insensitive to ν_μ and ν_τ (and water only weakly sensitive), so that the Homestake and Kamiokande rates are suppressed. Over the range of neutrino mass differences $\delta m^2 \sim 10^{-7} - 10^{-4}$ eV^2 and vacuum mixing angles $\sin 2\theta \sim 10^{-2} - 1$, the counting rate suppression can be just the required factor of 2 - 4. Neutrino magnetic moments, transition moments, neutrino decays, weakly interacting massive particles and nuclei with extra quarks in the solar core have also been invoked as possible causes of the solar neutrino problem.

So far only a radiochemical gallium experiment can provide the low background and low threshold required to study the flux of low-energy neutrinos from the fundamental proton-proton fusion reaction. The reactions in the p-p fusion chain, together with the neutrino energies and fluxes from the standard model calculations of Bahcall and Pinnseneault,[3] are shown in Fig. 1. In the standard solar model, in excess of 99% of the terminations of the proton-proton chain lead to emission of an electron neutrino with energy less than 0.42 MeV. ^{71}Ga, with a threshold of 0.23 MeV, is so far the only feasible target material capable of detecting the intense flux of these low-energy p-p neutrinos. Under the assumptions *i*) that the Sun is powered primarily by the PPI fusion chain ($p+p \rightarrow d+e^+ + \nu_e$, $d+p \rightarrow {}^3He+\gamma$, ${}^3He+{}^3He \rightarrow {}^4He+p+p$) and *ii*) that the rate of energy generation has remained constant over the 10^7 years required to transport energy from the solar core to the surface, the current observed energy output at the Sun's surface corresponds to a neutrino flux of 6×10^{10} cm^{-2}sec^{-1} from the p-p reaction alone. This conclusion is based largely on energetic grounds, and is insensitive to the details of solar model calculations. This p-p flux alone corresponds to a minimum expected counting rate in a gallium detector of 71 SNU. Based on the standard solar model calculations of Bahcall and Pinnseneault, the total counting rate in gallium, including all reactions, is expected to be 132 SNU, corresponding to 2 counts/day in a 60 ton experiment.

Two ^{71}Ga experiments are currently in operation. The first is the 60 ton Soviet American Gallium Experiment (SAGE) at Baksan,[9,10] which has recently reported a signal level of 73 +18/-16 (stat) +5/-7 (syst) SNU; the second is the 30 ton GALLEX experiment at Gran Sasso[11], which sees 87±14±7 SNU. Both results are consistent, and both suggest a neutrino flux level low compared to the total expected from standard solar model calculations. It is not possible, however, to make a case for flux levels lower than the p-p prediction. Assuming the experiments are correct (Neutrino source calibrations are planned for both SAGE and GALLEX in the near future.), it is not at all clear yet whether the answer lies with the neutrino physics, solar physics, or a combination of both.[12-14] Nevertheless, though solar model effects cannot be ruled out, if the Homestake and Kamiokande results are taken at face value, then these two experiments alone imply that neutrino oscillations or some similar particle physics result must be present to some degree.[13]

In Sec. II, the SAGE experiment and recent results are reviewed. LSU has been responsible for the low background proportional counter construction for the SAGE experiment, supported by DE-FG05-88ER40481. In Sec. III, non-radiochemical experiments are discussed, with an emphasis on the Kamiokande water Cerenkov results. Finally, the SuperKamiokande experiment is described, with a discussion of the proposed LSU plans for participation in SuperKamiokande, as the next step in our solar neutrino program.

II. Results from Prior DOE Support - SAGE Results and Future Plans

a. Recent Results

The SAGE detector, extraction and analysis procedures, and initial results have been described in Abazov et al. (Phys. Rev. Lett. 67, 3332, 1991) and most recently in Proc. Theory and Phenomenology in Astroparticle and Underground Physics (TAUP '93, Gran Sasso, to be published) and Physics Letters B, 1994, to be published. A full list of SAGE publications is given in Sec. IIe. We will therefore concentrate here on the recent results and the calibration work. With an initial 30 tons of gallium operated for the period January-July 1990, a 90% confidence upper limit was first obtained of $79/\xi$ SNU, where the efficiency factor ξ (assumed to be 1) is the ratio of extraction efficiency for neutrino-produced ^{71}Ge to that for the germanium carrier. The most recent result is 73 +18/-16 +5/-7 SNU. When combined with the GALLEX result of 87 ± 14 ± 7 SNU, this gives a weighted average of 81 SNU, corresponding to 62% of the Bahcall-Pinnseneault standard solar model.

Since the data runs described in the Phys. Rev. Letter, solar neutrino extractions were carried out on the 30 tons of original gallium from August through November 1990. However, due to the processing of the gallium for an engineering test run for a chromium calibration, backgrounds of radon and some ^{68}Ge in these data were substantially above the rate predicted by the standard solar model. Thus, it was not possible to use these data to improve the existing limits. Following the completion of the chromium engineering test run, a total of about 30 tons of new gallium was purified to remove ^{68}Ge (including further purification of the gallium used in the chromium test run). At the same time, the old gallium used in the previous solar neutrino runs was removed and the chemical reactors were extensively cleaned. The entire chemical extraction system was also carefully cleaned following completion of the purification of the new gallium. Tests in May of 1991 indicated that the levels of residual ^{68}Ge and radon were well below the signal predicted by the SSM. Separate extractions of the new and old gallium were carried out in June, July and August, 1991. Beginning in September 1991, combined extractions were begun on all 57 tons.

Figure 2 shows the observed counting rates derived from a likelihood analysis.* On the left is shown the rate for the first two mean lifetimes of the ^{71}Ge (τ_{Ge} = 16.5 days); on the right is the (predominately background) signal seen after the first two lifetimes. The progression from 1990 to 1991 to 1992 clearly shows both the systematic improvement in signal-to-background as the

* The analysis procedure is described in refs. [9,10].

experiment continues, and the statistical improvement as the gallium mass increased from 30 to 57 tons. A ^{71}Ge K-peak signal is clearly evident in the recent data.

A plot of the count rate per day in the K-peak region (Fig. 3) is consistent with the expected 16.5 day mean ^{71}Ge lifetime; and if we plot a histogram of the SNU values from the individual runs (Fig. 4), we find the observed distribution is consistent with the random Monte Carlo distribution calculated from the assumption of a mean value of 70 SNU. A summary of the results of the individual runs is shown in Fig. 5.

Intensive work has also been done to reduce noise pulsing and backgrounds in the L-peak. This effort includes rebuilding one of the counting systems with new preamplifiers, extensive filtering of all power lines, installation of a Faraday cage around the counting systems, improved passive shielding (including an improved radon purge), studies of noise reduction using data from a 1 Ghz transient digitizer, and installation of an additional stage of cryogenic distillation in the gas synthesis before filling of the counters. Analysis of the data with the upgrades indicates a reduction in the noise threshold by a factor of two to four and linearity in the electronics down to 500 eV. The electronic upgrades have now been completed, and we are now analyzing L-peak as well as K-peak data.

b. Low-Background Proportional Counters

The primary LSU responsibility has been the proportional counter construction: All SAGE counter building is now being done at LSU. The counter construction techniques rely on the use of clean materials, and are based closely on the experience gained in the Homestake experiment. The counter body (Fig. 6) is fabricated from Heraeus Amersil transparent synthetic fused silica (Suprasil). Suprasil has a total metallic impurity content of $\leq$1 part per million by weight (PPM) and OH and equivalent H_2O contents ~10^3 PPM. The counter bodies are blown by Karl Walther, formerly the glassblower responsible for the Homestake counters at Brookhaven. The seals and the thin calibration window are then checked with a helium leak test, and the counter bodies are cleaned by soaking overnight in aqua regia. After this acid bath, the final cleaning consists of a brief hydrofluoric acid etch and a thorough washing in high purity HPLC water. The counters are then dried in an oven at slightly above 100 C.

The main body of the counter is large enough to hold a snug-fitting zone-refined iron cathode sleeve. Again, care is taken to use only clean material: the cathode material typically has metallic impurities at levels less than 1 PPM; the only exception is copper, which is present at levels of ~7 PPM. The iron is drilled and cut to length in our machine shop using only new tools and HPLC hexane as lubricant. The cathodes, individually measured and machined to fit each individual counter body, are then washed in hexane in an ultrasound bath, baked and dried under vacuum for approximately 24 hours at 500 C, and handled only with gloves and clean tools. The cathode interior dimensions are approximately 5 mm diameter x 5 cm long.

Under a microscope, a 0.5 mil cathode wire of high-purity tungsten is spot-welded to the cathode and threaded through a thin capillary to the outside of the counter, where an external lead pin is connected. Again under a microscope, a 0.5 mil tungsten anode wire is threaded through a second capillary, through the center of the cathode sleeve, and welded to a 2 mil tungsten spring wire held in place at the end of the counter by a Suprasil endplug. With the anode and cathode wires held taut in the capillaries, the electrical connections to the external leads are made with a small dab of TRACON conducting epoxy injected into the end of the capillary through a hypodermic needle. The quartz endplug is gently welded in place by a glassblower with the wires still held taut, and then (with the counter filled with ~0.1 atm hydrogen to prevent oxidation of the thin wires) the capillaries are heated and sealed around the cathode and anode wires. The counters are then tested for gas-tightness, evacuated and baked for $\geq$72 hours, purged, and filled for testing with P-10.

Initial fabrication of the Suprasil parts is done by Walther at his shop in Florida, with the assembly and sealing being done in Baton Rouge. A graduate student (E. Young) and an undergraduate physics major (T. Whitt) have learned to do the anode construction and (together with M. Cherry) the spotwelding and wire installation. The final assembly, glass sealing, and testing are done by Cherry and C. Boussert, the LSU glassblower. Counter background rates measured at Baksan are in the range of approximately 1 count/day, with ~1 event/month in the ^{71}Ge K-peak region. Counters are tested at LSU for stability, gain, and resolution, but final background tests are performed underground at Baksan, where only counters with acceptably low background and noise counting rates are used.

c. Calibration and Efficiency Checks

After filling a counter with the GeH_4-Xe mixture from a gallium extraction, the counter is calibrated using an external ^{55}Fe source illuminating the central part of the counter through a thin side window. Calibrations are repeated at approximately one-month intervals. The stability of the counters in actual data runs is typically better than 5%. Possible polymerization of the wire due to repeated exposure to the ^{55}Fe source was checked by filling counters after the end of counting of the extraction samples with a fill of active $^{71}GeH_4$-Xe and calibrating the detector simultaneously with ^{71}Ge and ^{55}Fe. Any possible polymerization effects are negligible compared to the intrinsic counter stability.

The ^{55}Fe calibration is used to generate a two-dimensional plot of inverse rise time versus energy. A rectangular acceptance window is then calculated around the 5.9-keV ^{55}Fe peak which accepts 2 FWHM (98.15% acceptance) in energy (centered symmetrically around the ^{55}Fe) and 95% of the rise-time distribution, with 1% being cut on fast rise time pulses (i.e., noise) and 4% cut on the slow rise time peak (i.e. background). The position of the acceptance window for the ^{71}Ge K peak (at 10.4 keV) is calculated by first determining any electronic offsets using a linear pulser. The acceptance box for the ^{71}Ge K peak is then determined by scaling from the ^{55}Fe peak to determine the K-peak centroid in energy and inverse rise time, scaling the width in energy as the square root of the energy, and setting the width in inverse rise time to be constant and equal to the width for the ^{55}Fe peak.

In order to check this extrapolation procedure, a counter was filled with the standard GeH_4-Xe mixture in which the Ge was doped with ^{71}Ge. This provided an internal calibration source of ^{71}Ge in the counter gas with a total counting rate of less than 10 counts/s. All of the counting systems were calibrated using this counter. The spectrum from this counter taken simultaneously with the external ^{55}Fe source is shown in Figure 7. The acceptance boxes for the ^{55}Fe and the ^{71}Ge K peak are marked, and these data clearly show that the extrapolation method used is correct. The peaks occur all with the same rise time since they are all due to low energy Auger electrons and X rays that produce point ionization in the counter. Events with lower values of inverse rise time are due to background pulses that produce extended ionization in the counter while events with higher values are due to electronic noise and high-voltage breakdown in the proportional counters.

Numerous measurements have recently been carried out to determine efficiencies using counters filled with ^{37}Ar and $^{71}GeH_4$-Xe, which has resulted in a significant reduction in the systematic uncertainty of the counting efficiency. These measurements provided an absolute determination of the volume efficiency (the combination of dead volume in the counter and the effect of end losses due to fringing electric fields at the ends of the cathodes) with an accuracy of 3.2%. Monte Carlo calculations were then carried out to extrapolate the measured volume efficiencies with the gas fills used in the calibrations with ^{37}Ar and $^{71}GeH_4$-Xe to the different pressures and percentages of Xe used in the gas fills in the solar neutrino runs. This extrapolation introduces an additional uncertainty of 1%. Uncertainties in determining the centroid of the ^{55}Fe peak, in the ^{55}Fe ADP window, gain variations, and the extrapolation of the ^{55}Fe peak to the ^{71}Ge acceptance window result in an additional 3% uncertainty in the counter efficiency. Adding these uncertainties in quadrature gives a total uncertainty of 5.3% for the counting efficiency.

The systematic uncertainties of 3.7% and 5.3% of the chemical extraction and counting efficiencies, respectively, were added in quadrature together with uncertainties in the amount of Ga (0.5%), the exposure time (0.1%), the delay time between the extraction and the start of counting (0.5%), and dead time in the counting (0.5%) to obtain an overall uncertainty in the total efficiency of 6.5%.

A crucial remaining question, to be answered by a calibration experiment, is whether or not there exists some mechanism which could prevent efficient extraction and counting of ^{71}Ge atoms produced by inverse beta decay from solar neutrinos. The only physical mechanism we can envision would involve atomic or molecular excitations of the ^{71}Ge which would drive chemical reactions which would tie up the germanium in a form for which our chemical extraction procedure does not have high efficiency. A certain amount of information exists on this question, and a number of methods to provide this information have been suggested.

That atoms which have been produced in excited states can be extracted from metallic gallium has been demonstrated at some level during the cleanup of the gallium. Copious amounts of ^{68}Ge were produced by cosmic ray spallation in the gallium when it was on the surface. During the first extraction from 30 tons of gallium in 1988, the count rate in the K-peak acceptance window was 7700 events/day. Subsequent extractions reduced the count rate by about 80% per extraction, in line with the chemical extraction efficiency measured using the natural germanium carrier. At a very low level (roughly 1 ct/day in the K-peak), the extraction efficiency for ^{68}Ge became less than that of the natural germanium carrier. A reasonable explanation of this was that some small quantity of the ^{68}Ge had been absorbed into the Teflon liners of the gallium reactors when the ^{68}Ge concentration was very high and then was slowly released back into the gallium after the ^{68}Ge levels were reduced to a very small residual amount. However, it was impossible to demonstrate this conclusively due to the very low levels of residual ^{68}Ge involved. The possibility that some level of ^{68}Ge was chemically tied up in the reactors cannot be eliminated. Nonetheless, it appears that we efficiently extracted in excess of 99.9% of the ^{68}Ge.

As an additional test of the extraction process, we produced a sample of ^{71}Ge at Los Alamos and doped the natural germanium carrier with a known quantity of radioactive ^{71}Ge. The doped carrier was added to one of the reactors holding 7 tons of gallium, and three successive extractions were carried out. For each extraction, the number of ^{71}Ge atoms was counted. A total of 525 ± 26 μg of carrier were added, corresponding to 6555 ± 359 decays expected. Table 1 shows that the extraction efficiency of the carrier and the ^{71}Ge counting tracked very closely.

We have carried out a third set of measurements designed to address this question, as well. In this experiment, we have taken a few grams of gallium from the Baksan reactor vessels and then have done 6 extractions to remove all of the residual Ge carrier. The gallium was then irradiated in the Missouri Research Reactor. ^{70}Ga and ^{72}Ga are formed from ^{69}Ga and ^{71}Ga respectively by (n,γ) reactions. The natural abundances of ^{69}Ga (60.1%) and ^{71}Ga (39.9%) coupled with the thermal neutron capture cross sections for ^{69}Ga (1.7 barns) and ^{71}Ga (4.6 barns) result in the production of a few micrograms of ^{70}Ga and ^{72}Ga per gram of irradiated natural Ga. The ^{70}Ga and ^{72}Ga subsequently decay to stable ^{70}Ge and ^{72}Ge with half-lives of 21.1 min and 14.1 hrs respectively. Table 2 shows the decay energies and branches. The gallium metal is kept liquid (in order to simulate the conditions in the solar neutrino runs) and allowed to sit for a few weeks so that all of the ^{70}Ga and ^{72}Ga have decayed. The stable ^{70}Ge and ^{72}Ge are then extracted, and both the absolute amounts and the ratio are determined by mass spectroscopy.

Invoking the sudden impulse approximation, the dominant effects upon atomic excitation and ionization are due to the sudden change in Coulomb charge and are independent of whether the sudden change in Coulomb charge is due to beta decay or inverse beta decay. Thus, we expect measurements of the extraction efficiency from the Ga (n,γ) experiments to directly test the hypothesis that some exotic chemistry binds the germanium in a form which we cannot efficiently extract. Mass spectrometric measurements indicate that the natural germanium carrier was removed from the gallium (as expected) during the purification and that we find a $^{70}Ge/^{72}Ge$ ratio of 0.55 compared to the expected value of 0.52. Extraction efficiencies were 92-98%.

While the removal of the cosmogenic ^{68}Ge from the gallium and the Ga (n,γ) measurements can provide us with good confidence that nothing is inherently wrong in our extraction procedures, it is still essential to carry out a full-scale ^{51}Cr calibration. Only by carrying out the ^{51}Cr experiment can we demonstrate that the full scale system is operating quantitatively as expected even with small numbers of germanium atoms, and that in fact our observation of low numbers of extracted ^{71}Ge atoms does indeed show that there is a deficit of low energy solar neutrinos. ^{51}Cr provides an almost ideal source of neutrinos with which to calibrate the gallium experiment. ^{51}Cr

Table 1. Extraction Efficiency of Germanium Carrier and ^{71}Ge.

Run	Carrier (μg) extracted	^{71}Ge atoms detected	Efficiency Carrier	Efficiency ^{71}Ge
1	410 ± 10	5188 ± 195	78 ± 4%	79 ± 5%
2	97 ± 2	1131 ± 107	84 ± 20%	84 ± 26%
3	21 ± 1	<200		
Sum	528 ± 10	6519 + 222/-422	101 ± 5	99 + 6/-8

Table 2. Principal Decays of ^{70}Ga and ^{72}Ga

Isotope	Decay Mode	Decay Energy (MeV)	Branching Ratio
^{70}Ga	β^-	1.6563	99.3%
	e^- capture	0.6548	0.2%
^{72}Ga	β^-	3.1577	11.0%
	β^-	2.5277	8.0%
	β^-	1.9267	3.0%
	β^-	1.4769	9.0%
	β^-	0.9560	28.0%
	β^-	0.6666	21.0%
	β^-	0.6500	14.9%

Table 3. Decay Scheme of ^{51}Cr

Neutrino Energy	Branching Ratio
751 keV	9%
746 keV	81%
431 keV	1%
426 keV	9%

decays by electron capture with a half-life of 27.7 days by either

$$^{51}Cr + e^- \rightarrow {}^{51}V + \nu_e \qquad (BR=90\%)$$

or

$$^{51}Cr + e^- \rightarrow {}^{51}V + \nu_e + \gamma \qquad (BR=10\%)$$

The decay scheme of ^{51}Cr is given in Table 3, which includes the effect of the 5 keV atomic excitation in the K shell. A 320 keV gamma ray is emitted simultaneously with the 431 and 426 keV neutrinos. The neutron capture cross section is 15.9 barns, making it possible to make an intense ^{51}Cr source by irradiating ^{50}Cr with thermal neutrons.

An engineering test run with a lower intensity ^{51}Cr source was carried out during the fall of 1990. A primary difficulty for the test run was an extended shutdown of the production reactor in October, 1990 for reactor upgrades, scheduled with only a few months advance warning. Thus, the test run was mounted in a period of only three months, which did not allow us time to prepare everything in the same final form as planned for the full scale calibration run. Nonetheless, it was decided that valuable operating experience would be gained by carrying out an engineering run with a lower intensity source. A source was produced at the SM-2 reactor in Russia by irradiating 212 gms of 87.7% enriched ^{50}Cr in a thermal neutron flux of 2 x 10^{15} n/cm^2/s. Due to time constraints, only part of the chromium was both chemically purified and then zone refined, while the remainder was only chemically purified. Various samples of the chromium were irradiated for different periods during an 80 day period. Some of the irradiated chromium suffered damage from embrittlement and the rods fractured. However, the majority of the irradiated chromium rods (total mass of 200 gms) were inserted into a stainless steel cylinder, which was then placed inside a depleted uranium shield with 15 mm thick walls to make a compact source of 74 mm diameter by 134 mm high. The source was then transported to the underground laboratory at Baksan. The total ^{51}Cr source activity was determined by thermal calorimetric measurements to have been 351 kCi on October 18, 1990 when the source was first placed in the gallium. The level of high energy gamma radioimpurities with half-lives of several weeks or longer was determined by measurements made during January 1991 with a high purity germanium detector to be about 0.4%.

Five consecutive irradiations of approximately 12 tons of gallium were made. For the first three exposures, newly purified gallium was used, while the last two exposures used old gallium from the solar neutrino runs. The normal procedure used was to mix natural Ge carrier into two gallium reactors and then to pump gallium from these two reactors into a single reactor in which the stirrer has been replaced by a reentrant port for the chromium source. The gallium was irradiated for periods of 12 to 18 days. It was then pumped back to the two original reactors and extractions were then carried out on these two reactors. Any ^{71}Ge produced was counted using the same counters and electronics as used in the solar neutrino runs. The chemical extraction efficiency using this process was measured to be the same as that typical for the solar neutrino runs.

Since only one chemical extraction system existed, this system was used to purify the new gallium, to purify the reagents, and to continue solar neutrino runs. As a result, due to the short preparation time for the test run, the new gallium had not been entirely purified of residual ^{68}Ge and the reagents were not purified to the same purity level as used during previous solar neutrino runs. This resulted in backgrounds in the test run an order of magnitude higher than in the previous solar neutrino runs. The dominant components of the background were ^{68}Ge and radon. Only the first four extractions were counted, while the fifth extraction was used to check radon levels in the extraction. While the runs indicated some apparent production of ^{71}Ge, due to the high background and the presence of radon it was not possible to determine a reliable quantitative measure of the production rate of ^{71}Ge. Nonetheless, a great deal of valuable experience from handling a few hundred kiloCurie source and in determining the technical problems involved in a calibration measurement was obtained.

d. Full-Scale ^{51}Cr Calibration

At this point, we expect to continue normal solar neutrino runs with 57 tons of gallium and extractions on a monthly basis until a full-scale (0.5 MCi) chromium calibration begins later this year. However, we will modify our solar neutrino runs in the two to three months prior to the calibration experiment in that approximately 14 tons of gallium will be used in the chromium irradiation reactor and extracted and counted separately from the remaining 43 tons of gallium. Once irradiations with the ^{51}Cr source begin in the chromium irradiation reactor, solar neutrino runs will be stopped for the duration of the calibration experiment. This halt will be for two reasons. First, we want to concentrate our efforts on the ^{51}Cr runs in order to ensure success. And second, this halt is required since there will be production of ^{71}Ge in reactors adjacent to the chromium irradiation reactor at levels comparable to the Standard Solar Model production rate. In fact, we plan to try to measure this production since this will be under conditions identical to solar neutrino running. Although the statistical accuracy will be poor, it will at least demonstrate consistency with our solar neutrino data. The source (to be produced by irradiating a 300 g sample of 90% enriched ^{50}Cr in the BN-350 fast neutron reactor in Russia) will be transported to the underground laboratory at Baksan and placed in a reentrant port in the tank with the 14 tons of gallium metal. A series of six extractions will be made at 2-week intervals. In all, we expect a total of approximately 600 atoms of ^{71}Ge to be produced; about 240 K- and L-decays should be observed, yielding a statistical accuracy of better than 10% after background subtraction. Systematic uncertainties are expected to be ~10%, yielding an overall precision of 14%.

Calculations indicate that the gamma activity at a distance of 1 m from the shield should be less than 1 mR/hr, assuming that radioimpurities can be kept to the ppb level. The source assembly will be transported in a large lead shield which has a sliding trap door on the bottom. The source can be removed by inserting a rod with a lock pin through a small hole in the top of the lead shield, opening a trap door on the bottom of the lead shield, and lowering the source. Although we are striving to produce a source which will have minimal levels of external radiation, prudence and good safety practices require that we should not have to directly handle the source. Thus, we are planning to install a remote handling capability at the experiment to carry out the operations of source transfer and installation. The procedures requiring remote handling are rather minimal so that only a fairly simple remote handling capability is required. The operations to be performed at the experiment are 1) transfer of the source from the lead shipping shield and installation and removal of the source in the reentrant port of the reactor containing the gallium, 2) installation and removal of the shielding in the reentrant port above the source, 3) removal of the source from the reentrant port after the irradiation, 4) transfer of the source to the calorimeter used to determine the total source activity, and 5) transfer of the source to a highly collimated shield to allow measurements of radioimpurities by measuring high energy gammas emitted by the source with a hyperpure germanium detector. A fairly simple hydraulically operated remote arm equipped with television cameras will be adequate to handle all of the above requirements. The source shields will be designed to be compatible with the remote handling equipment. The only operation which will require some modifications to existing equipment is the transfer of the source to the calorimeter. This will involve some minor modifications to the removeable shielding and the internal covers of the calorimeter. Training of two operators will be carried out using dummy loads prior to operation with the ^{51}Cr source.

There are two techniques which will be employed to determine the total source intensity. The first is by direct counting of the gamma activity from the source and the second is by thermal calorimetry. Direct counting of gammas from the source presents a number of difficulties in determining the absolute source intensity. Since the irradiated chromium is in the form of single crystal rods, it is not possible to mix all of the irradiated sample together to assure uniformity and then to remove a small sample to determine the source intensity by counting the 320 keV gammas emitted in the decay of ^{51}Cr. We are constrained to measure the source intensity after the chromium rods are inside the HeviMet shield. Thus, one must do systematic measurements covering all directions from the source and Monte Carlo the number of gammas which will escape through the HeviMet shielding. It is unlikely that this can be done to better than 20-30% accuracy. However, it is quite important to carry out this measurement in order to determine the level of radioimpurities which emit high energy gamma rays from the source in order to correct the calorimeter measurements.

A 1 MCi ^{51}Cr source emits 217 W of thermal power due to the 320 keV gammas in the decay. A passive thermal calorimeter was developed and tested during the engineering test run by I.N. Belousov of the All Union Scientific Research Institute of Metrology. It proved to have a precision of about 1 ppm during a 15 minute measurement. This sensitivity is not only sufficient to determine the total source activity, but also allows a very precise measurement of the decay time of the source. This in turn provides the necessary information to correct for radioimpurities which contribute to the thermal power of the source. The overall accuracy of the calorimeter measurements achieved in the engineering test run was ±2%, which includes both statistical and systematic effects. The level of accuracy expected in the full scale engineering test run is expected to be approximately the same, or slightly better as the level of radioimpurities is expected to be under better control.

It is not feasible to carry out the calibration experiment in exactly the same manner as the solar neutrino runs, due to the method used for chemical extraction. Thus, we plan to pump gallium from two reactors into a special third reactor which has a zirconium reentrant port in it. The irradiations will be made in this special reactor which will hold approximately 14 tons of gallium. The procedure to be used is as follows. Isotopic germanium carrier will be added to two of the reactors, each holding 7 tons of gallium, and the gallium will be stirred to thoroughly mix the carrier. The gallium will then be pumped to the chromium irradiation reactor and the ^{51}Cr source inserted into the reentrant port. After an irradiation, the gallium will then be pumped back to the two original reactors and chemical extraction of the germanium will be carried out using exactly the same procedure used in solar neutrino runs. The efficiency of this approach was checked during the engineering test run in which it was demonstrated that the carrier extraction efficiency in this scheme was the same as in the solar neutrino runs. In order to further check this procedure, we plan to carry out two or three runs on solar neutrinos using the chromium irradiation reactor. While the statistical accuracy with 14 tons will be considerably less than in our normal solar neutrino runs with 30 or 60 tons of gallium, it should still be consistent with our normal solar neutrino runs. We plan to carry out 6 irradiations with the ^{51}Cr source with extractions from the 14 tons of gallium being carried out every 2 weeks. At the end of these irradiations (84 days after the start), the production rate of ^{71}Ge will be down to less than one ^{71}Ge atom per day.

The counting techniques will be identical to those used in our normal solar neutrino runs. However, in order to check possible systematics, a number of blank runs and second extractions will be carried out which will require more counting channels and counters. We expect to have three samples per extraction, from the first extraction, the second extraction, and one blank. At present we have only counters to carry out normal solar neutrino runs. Thus, additional counters are presently being constructed for the calibration experiment.

The data from the ^{51}Cr calibration experiment will be analyzed in exactly the same manner as the solar neutrino runs. The maximum likelihood analysis will provide a best fit number for the number of ^{71}Ge atoms produced. This number will be compared with Monte Carlo calculations in order to determine the extraction efficiency. Given the high decay rates, at least in the first extraction, we expect to be able to count both the K- and L-peaks in the ^{71}Ge decay. Even if we are able to count only the K-peak, as in our initial solar neutrino running, a statistical accuracy of about 15% should still be achieved. In this case, we expect to be able to achieve an overall precision of 20% including systematic uncertainties.

e. SAGE and Related Publications Since 1990

1. "The Baksan Gallium Solar Neutrino Experiment," V. N. Gavrin et al., in Inside the Sun, eds. G. Berthomieu and M. Cribier, (Dordrecht, 1990, Kluwer Academic Publishers), pp. 201.

2. "The Soviet-American Gallium Solar Neutrino Experiment: A Status Report," V. N. Gavrin et al., Proc. 21st Intl. Cosmic Ray Conf., Adelaide, Australia, 7, 179 (1990)
3. "Measurement of Solar Proton-Proton Fusion Neutrinos with a Soviet-American Gallium Experiment," M. L. Cherry, invited highlight paper, Proc. 21st Intl. Cosmic Ray Conf., Adelaide, Australia, 12, 152 (1990).
4. "Neutrino Oscillations and Solar Models," C.X. Chen and M.L. Cherry, Ap. J. Lett. 377, L105 (1991).
5. "First Results from the Soviet-American Gallium Experiment," A.I. Abazov et al., Nucl. Phys. B 19, 84 (1991).
6. "Search for Neutrinos from the Sun Using the Reaction $^{71}Ga(\nu_e,e^-)\,^{71}Ge$," A.I. Abazov et al., Phys. Rev. Letters 67, 3332 (1991).
7. "Measurement of the p-p Solar Neutrino Flux by the Soviet-American Gallium Experiment," A.I. Abazov et al., Proc. 22*nd* Intl. Cosmic Ray Conf., Dublin 3, 724 (1991).
8. "The Solar Neutrino Problem: Neutrino Physics vs. Solar Physics," C.X. Chen and M.L. Cherry, Proc. 22*nd* Intl. Cosmic Ray Conf., Dublin 3, 744 (1991).
9. "Results from the Soviet-American Gallium Experiment," A.I. Abazov et al., Proc. Intl. Workshop on Electroweak Physics Beyond the Standard Model, Valencia, Spain, (1991).
10. "Results from the Soviet-American Gallium Experiment," O.L. Anosov et al., Proc. Fourth Intl. Workshop on Neutrino Telescopes (Venice), ed. M. Baldo Ceolin, p. 39 (1992).
11. "Latest Results from the Soviet-American Gallium Experiment," V.N. Gavrin et al., Proc. Intl. Conf. on High Energy Physics, Dallas (1992).
12. "Status of the Soviet-American Gallium Experiment," O. L. Anosov et al., Proc. Texas PASCOS Conf., Berkeley (1992).
13. "Results from the Soviet-American Gallium Experiment," O. L. Anozov et al., Nucl. Phys. B 31, 111 (1993).
14. "Results from SAGE (The Russian American Gallium Solar Neutrino Experiment)," J. N. Abdurashitov et al., Physics Letters B, to be published (1994).

III. Electronic Solar Neutrino Experiments

In addition to checking and refining the gallium results, there are three main experimental directions for further progress:

1. measurement of the ^7Be neutrino flux;
2. direct observation of a neutral current contribution; and
3. improved measurement of the ^8B recoil electron spectrum.

In addition, positive observation of time variations and/or a high energy hep component will be extremely interesting, but these studies will come naturally as part of items 1 -- 3. Three major new solar neutrino detectors designed to address these specific issues are currently either under construction or in advanced planning stages: Borexino, SNO, and SuperKamiokande. These detectors are described below. As described in Sec. IIIc below, SuperKamiokande in particular will have the capability to do a definitive measurement of the ^8B spectrum, and should be able to differentiate conclusively between the neutrino oscillation solutions compatible with the current chlorine, water, and gallium results.

The experiments will also have extremely high sensitivity for a galactic supernova neutrino burst. The supernova neutrino burst capabilities have been described elsewhere[5,15,16] and are not described in detail here for the sake of brevity.

a. Liquid Scintillator -- Borexino

Borexino will be a 300 ton liquid scintillator experiment at Gran Sasso designed to observe ^{7}Be neutrinos via ν - e scattering.[15] The expected signal in a 100 ton fiducial volume (assuming the Bahcall -- Pinnseneault standard solar model) is 1-2 events/hr with electron recoil energies above 250 keV. Assuming backgrounds due to radioactive impurity levels can be controlled (at levels of 10^{-16} - 10^{-15} grams of uranium and thorium per gram of scintillator), this rate should be sufficient to see a yearly variation in the solar signal due to the $1/R^2$ variation of the earth's orbit about the Sun.

b. Heavy Water -- SNO

The Sudbury Neutrino Observatory (SNO) will be a 1000 tonne D_2O Cerenkov detector to be located in Sudbury, Ontario.[16] SNO will be sensitive to ^{8}B and hep neutrinos via the charged current $\nu_e + d \rightarrow p + p + e^-$ reaction at a rate of 3000/yr (assuming 1/3 the flux of Bahcall and Pinnseneault's standard solar model), *all* neutrinos above 2.2 MeV via the neutral current $\nu_x + d \rightarrow \nu_x + p + n$ reaction (also at ~3000/yr assuming the full standard solar model flux and assuming neutron backgrounds can be managed), and ν_e with directional sensitivity but a lower rate (~300/yr assuming 1/3 the standard solar model rate) via ν_e elastic scattering.*

c. Light Water -- Kamiokande and SuperKamiokande

SuperKamiokande, with a 32,000 ton sensitive volume of light water, will see ~2500 events/yr above ~7 MeV from the direction of the Sun. The directional sensitivity makes it possible to tag true solar events and measure the energy spectrum of tagged ^{8}B (and hep) solar neutrinos with excellent statistics. The procedures, capabilities, and actual background levels have been well demonstrated with Kamiokande II and III.[5] We review the Kamiokande results here and describe the proposed SuperKamiokande instrument (and the LSU role in the experiment) in more detail in Sec. IIIc2.

1. Kamiokande Performance and Results. Kamiokande is a 4500 ton, 16 m high x 19 m diameter cylindrical water Cerenkov detector instrumented with 948 50 cm diameter photomultiplier tubes. Located at a depth of 2700 mwe, the instrument has a solar neutrino fiducial volume of 680 tons. The experiment has been operating, looking for proton decay, supernova neutrino bursts, atmospheric high energy neutrinos, magnetic monopoles, n-$\bar{n}$ oscillations, and solar neutrinos, since 1983. With 20% photocathode coverage, 1 MeV corresponds to approximately 5 detected photoelectrons; the result is a capability of triggering at a threshold near 7.5 MeV.

An important issue for determining efficiency, energy resolution, directional response, and background rejection capability is the calibration. The energy calibration is performed in three independent ways: by using the 9 MeV γ rays from an artificial ^{252}Cf - Ni source, the electrons from stopping muon decays, and the β decays from radioactive nuclides produced by spallation induced by cosmic ray muons. In all cases the measured results were compared to the output of Monte Carlo simulations, and in all cases the detailed agreement was excellent. For the energy calibration, the comparisons gave consistent agreement within 3%, leading to a quoted uncertainty in the absolute energy scale of less than 3% and an approximate energy resolution (after the June 1988 doubling of the photomultiplier tube gain) given by

$$\sigma(E_e)/E_e = 0.63/\sqrt{E_e}\,.$$

The gain was measured to be stable to within 2% over four years of operation. Angular resolution was measured with the Ni(n,γ)Ni* source at the top of the detector, with a resulting measured

* The ν - e scattering process also has sensitivity to ν_μ, but with a cross section a factor of ~6 lower than for ν_e.

angular resolution ranging from 38° at 5 MeV to 21° at 20 MeV. Timing is calibrated using a nitrogen gas laser to illuminate a diffusing ball at the center of the detector.

The major backgrounds in the Kamiokande experiment are produced by radioactivity in the water, γ rays and neutrons from the rock outside the detector, and β's from the decays of radioactive nuclei produced by spallation in the water. The largest contributor to the trigger rate below 7 MeV is ^{214}Bi born as a daughter of ^{222}Rn with a β spectrum endpoint of 3.26 MeV. ^{222}Rn is present in the mine water at levels of 200 - 300 pCi/liter and in the mine air at a concentration of ~50 pCi/liter. Kamiokande went to great lengths to remove uranium, ^{226}Ra, and radon by installing a water purification system employing dual ion exchange columns, by sealing the top cover of the detector and the circulation/purification system, by injecting radon-free gas into the system, and by adding a degasification system. The result of these efforts was to reduce the ≥7.5 MeV trigger rate in the fiducial volume to 5 events/day. The detector is currently triggering at a threshold of 5.2 MeV.

The flux of external γ rays and neutrons is reduced by $\sim 10^3$ by the anticoincidence layer shielding. Remaining external events penetrating the shield typically interact in the outer portions of the detector, and are typically moving inward. These are reduced by an additional factor of ~400 in the data analysis, leaving a residual solar neutrino background due to external γ's of 1 - 2 events/day.

At the Kamiokande depth, the rate of cosmic ray muons penetrating the detector is 0.37/sec. These high energy muons fragment oxygen nuclei in the water; stopping μ^- are captured by ^{16}O to produce ^{16}N; and π^- capture by ^{16}O leads to ^{12}B and ^{12}N. The resulting β decays typically occur near the tracks of the incoming muons with time delays $\Delta T \leq 20$ sec. Muon-induced spallation background is recognized in the data analysis with an efficiency of 90 - 95%, leading to a reduction in the event rate above 10 MeV by a factor of 4 - 5 and a resulting dead time of 17%.

Data are selected by requiring only a small anticounter pulse height (to remove events coming in from the outside), a minimum 10 μsec delay after the previous event (to reject decay electrons from μ decay), and a recoil electron energy $E_e \leq 30$ MeV. The event location is determined and required to lie within the inner fiducial volume of the detector; and spallation backgrounds and external γ rays are rejected in the data analysis.

The next step is to plot the recoil electron angular distribution, shown in Fig. 7 together with the expected distribution based on the Bahcall-Pinnseneault standard solar model prediction. The peak in Fig. 7 gives a clear indication of an excess signal *from the direction of the Sun* corresponding to a flux

$$0.50 \pm 0.04\ (\text{stat}) \pm 0.06\ (\text{syst})$$

times the flux calculated by Bahcall and Pinnseneault. The observed recoil electron energy distribution for events from the direction of the Sun (i.e., for events with $\cos\theta_\odot \geq 0.9$) is shown in Fig. 8. The solid curve is the expected distribution. The data points are well fitted by the predicted curve scaled down by an overall (energy-independent) suppression factor as shown by the dashed curve.

2. *Solar Neutrino Measurements in SuperKamiokande.* Assuming SNO can reduce its neutron backgrounds sufficiently, the Sudbury D_2O detector will have the capability to measure the neutral current contribution to the solar neutrino rate and therefore provide a direct measurement of solar neutrino oscillations. SuperKamiokande will provide complementary information by measuring the ^{8}B recoil electron spectrum. It should be noted that SNO has the capability to measure the spectrum as well, but if one restricts the analysis to the directional component that is clearly coming from the sun, then the ν - e elastic scattering rate in SNO will be ~300/yr compared to 2500/yr (above 7 MeV) in the 22,000 tonne SuperKamiokande inner fiducial volume.

Assuming MSW oscillations and a neutrino production rate given by the standard solar model predictions, the regions of δm^2 - mixing angle space that are consistent with Homestake, Kamiokande II, and gallium are shown in Fig. 9. Along the upper (horizontal) portion of the triangular region allowed by the ^{8}B experiments, the suppression of the flux due to MSW oscillations is primarily at high energies. Along the right-hand (vertical) section, the oscillations are essentially energy-dependent. And along the diagonal section, the suppression is at low energies. If the gallium results are added in, one is restricted to two regions near the upper right and upper left of the triangle, as shown in more detail in Fig. 10.

Given the limited statistical accuracy of the Kamiokande II electron spectrum results, both of these solutions are currently possible. With better statistics, however, one could both see the expected signal in the spectrum and differentiate between the left-hand solutions (with suppression at lower energies) and the right-hand solutions (with energy-independent suppression). In Fig. 11 we show the spectra expected for a set of solutions consistent with Homestake, Kamiokande II, and gallium. The SuperKamiokande statistical error bars will be sufficiently small to distinguish between the alternatives; for comparison, the typical Kamiokande II error bars (also shown on Fig. 11) are much too large to permit such a detailed study.

i. Detector Description. In order to provide the statistics and sensitivity necessary to measure the ^{8}B solar neutrino recoil electron energy spectrum sufficiently accurately, and at the same time provide an order-of-magnitude improvement in nucleon decay lifetime sensitivity, SuperKamiokande will be almost 8 times the size of the IMB-3 detector and have a factor of 7 increase in light collection capability. SuperKamiokande is designed to be a 50,000 ton ring-imaging water Cerenkov detector to be constructed at a depth of 2700 meters water equivalent (mwe) in the Kamioka Mozumi mine in Japan. A schematic representation of the detector is shown in Fig. 12. It consists of a stainless steel tank in the shape of a right circular cylinder, 39 m in diameter and 41 m high, filled with purified water. The detector is optically segmented into an inner volume (34 m diameter, 36 m height) and an outer (anti-coincidence) region of 2.5 m thickness on top, bottom, and sides of the inner volume. The inner detector is viewed by 11,200 photomultiplier tubes (PMTs) of 50 cm diameter, uniformly distributed on the inner boundary giving a 40% photocathode coverage. This extraordinary photocathode coverage and time resolution (2.5 ns at 1 p.e.) allows the detector to attain an energy threshold of 5 MeV and a vertex resolution of 10 cm for processes such as $p \rightarrow e^{+} \pi^{0}$. For through-going muons, the PMT configuration yields an angular resolution of 1°. The total mass of water inside the inner detector PMT surface is 32,000 tons. The fiducial mass for the proton decay search, defined to be 2 m inside the PMT plane, is 22,000 tons allowing for partial lifetime sensitivities of $\geq 10^{34}$ years for several modes.

The outer annulus of the detector is an anti-coincidence region used to tag entering muons and low energy components as well as to attenuate low energy gammas and neutrons which cause background in the sensitive volume. It also complements calorimetry in the inner detector by measuring the energy loss due to exiting particles. This outer detector region is viewed by 2200 PMTs of 20 cm diameter with wavelength shifter plates in the style of IMB-3. The walls of the anti-coincidence region are made reflective to enhance light collection. The PMTs are mounted facing outwards on the same super-structure as the 50 cm PMTs of the inner volume. Also, an optical barrier is mounted on the same structure to separate the inner and outer regions.

After construction, the tank will be sealed by a painted carbon steel top which will prevent the entry of radon gas, a serious problem in the Mozumi Zinc Mine. Plans call for continuous operation for 5 years before opening the tank for maintenance. Five electronics huts containing the readout electronics will sit on top of this lid. A fiber optic link to a laboratory now being built outside the mine allows for remote operation.

The major responsibility of the American contingent of the collaboration is to construct the anti-counter. The shutdown of the IMB detector makes available about 2,000 20-cm Hamamatsu PMT's (worth about $2 M) for this task. The U.S. SuperKamiokande construction proposal (now approved by DOE High Energy Physics) describes the initial design studies for the anti-counter. Its main purpose is to aid in separating "contained" events (neutrino interactions or nucleon decays) from the 3 Hz cosmic ray muon background. IMB had no such anti-counter and thus had problems in reducing the data and telling if energy was "leaking" out of the detector, or leaking in from muon-induced gamma rays from the surrounding rock. Figure 13 shows a rough diagram of the planned anti-counter.

ii. LSU Responsibilities. At LSU, the faculty involved in SuperKamiokande will be M. Cherry and R. Svoboda (who previously worked on the IMB experiment), together with postdoc Mark Vagins. Since it is planned that SuperKamiokande will take a very large quantity of data (estimated at about 5 Gbyte/day), it is necessary to have a real-time data monitoring system to ensure that the data being collected is usable. To do this, we plan to develop the software at LSU for a DAQ Monitor to perform such tasks as:

1. Calculating angular distribution and timing residuals of cosmic-ray muon fits. These are a very good "bottom line" monitor of data quality: If something went wrong in IMB it usually showed up here first;
2. collecting PMT TDC and QDC spectra for individual tubes, for comparison with baselines;
3. collecting PMT dark noise rates, for comparison with baselines;
4. evaluating the performance of individual trigger schemes;
5. on-line sensing of PMT failures; and
6. monitoring of tank water levels, temperatures, etc.

The lack of a sophisticated data monitoring system in IMB due to computer processing limitations was sorely felt in the live-time/duty-time fraction, which was about 50-60%. We would like SuperKamiokande to operate with a duty time of >90%; an on-line data monitoring system will be especially crucial to our final nucleon decay and supernova burst sensitivity.

The development of the DAQ monitoring system will begin this year with the purchase of two SUN computers from DOE construction funds. Specifications for such a system are being written by Svoboda in consultation with M. Nakahata from U. Tokyo (in charge of read-out electronics for the central detector). A DAQ system mock-up will be built at LSU that mimics the SuperKamiokande data stream in one computer, while the other will serve as the DAQ monitor computer which is to hang in a parasitic fashion on the FDDI link. The specifications call for the ability not only to monitor data from this computer, but also for other computers to establish real-time links with it outside the mine (such as at LSU!) to monitor detector performance remotely. This software task is formidable but must be completed early on in order to debug the whole data acquisition system prior to *in situ* PMT testing. Since this means we must have the complete system before the end of 1995, we must start this year. We therefore propose to hire a software technician proficient in SUN/UNIX/FDDI to begin in early 1994 and continue through task completion in 1995.

The second main task at LSU will be the anti-counter photomultiplier tube, cable, and base assembly and testing operation. We hope that it may be possible to use the old IMB bases with a few modifications. These modifications would:

- replace any remaining carbon film resistors, which have a low MTBF;
- change the voltage dividing scheme of the divider chain to increase the dynamic range of the base for high energy muons.
- solder the HV and signal lines directly to the base; and
- replace one or more of the final stage capacitors, also to increase dynamic range.

In what could have a major impact on base design, it now seems possible that we will have to remove the IMB PMT's from their PVC housings due to radon problems with PVC. In this case, a study will have to be done to see if it is possible to pot the bases in some insulating material (as is being done with the 50-cm PMT's) without inducing heat dissipation problems that could hurt later. The other option is to look for non-radon producing PVC and build new housings, but this would probably be more expensive in the long run.

At LSU, we have just begun planning the design of a modified base with B. Ellison from our electronics shop and S. Khosrovi, our technician who will supervise the fabrication and piece-by-piece testing of the bases. We plan to set up the test stand early in 1994 and begin fabricating bases during the summer.

For cables, the original construction proposal called for us to purchase the same ones being used for the 50-cm PMT's by the Japanese. The old IMB cables are not only too short (by a good 30 meters!) but also were the cause of many PMT failures. They were not "flooded" cables (i.e., cables filled with a waterproof filler). Thus a nick or hole in the outer jacket meters away from a PMT would eventually cause the housing to flood by water wicking through the cable. Though the Japanese solved this problem by using a flooded cable, their cable is quite expensive and suffers from noise pick-up due to the fact that it is a dual-conductor with the HV line unshielded. Therefore, we have obtained sample cables from manufacturers in the U.S. which combine the noise protection aspects of the old IMB cables with the flooded design of the Japanese ones. Such cables can be obtained MUCH more cheaply (about a factor of 2-3!) due to the fact that flooded cables are now used in the cable TV industry. The samples we have are not susceptible to noise pick-up because they are of single-shielded conductor design. Of course, this solution is a trade-off, since we would then have to build signal pick-off cards similar to the ones used in IMB, but we still believe the bottom line price will be less with better performance.

The planned SuperKamiokande construction schedule for LSU is as follows:

- **1993-94:** Calibration beam test at KEK (Svoboda, Vagins, and Cherry). Begin work on detailed detector simulations and combine them with updated IMB atmospheric neutrino models (Vagins, Svoboda). Put together test set-up and complete PMT base and cable design (Cherry, Svoboda, Ellison, Khosravi). Prototype them, test, and begin fabrication (Cherry, Ellison, Khosrovi). Complete specification and begin design of DAQ monitoring system (Svoboda, Programmer).
- **1994-95:** Finish detector simulation software and convert IMB data reduction software to SuperKamiokande use (Vagins, Svoboda). Complete DAQ monitoring system and send to experimental site for debugging (Svoboda, Programmer). Complete base and cable fabrication and ship to UCI for mating with PMT's (Cherry, Khosrovi). Begin work on calibration system control software with U. Hawaii and U. Wash (Svoboda).
- **1995-96:** Complete calibration control software (Svoboda). Begin detector assembly in Japan, with LSU postdoc resident there during this period and others going for extended construction shifts.
- **1996-97:** Taking data.

References

[1] Davis., R. *et al.*, 1990, Proc. 21st Intl. Cosmic Ray Conf., Adelaide, **7**, 155; Rowley, J.K. *et al.*, 1985, in *Solar Neutrinos and Neutrino Astronomy* (AIP Conf. Proc. No. 126), ed. by M.L. Cherry *et al.*, p. 1.
[2] Davis, R., 1993, Proc. 23rd Intl. Cosmic Ray Conf., Calgary **3**, 869.
[3] Bahcall, J.N. and Ulrich, R.K., 1988, Rev. Mod. Phys. **60**, 297; Bahcall, J. N. and Pinnseneault, M. H., Rev. Mod. Phys. 1992, **64**, 885.
[4] Turck-Chieze, S. *et al.*, 1988, Ap. J. **335**, 297.
[5] Hirata, K.S. *et al.*, 1991, Phys. Rev. D **44**, 2241; 1990, *Phys. Rev. Lett.* **65**, 1297; 1990, *Phys. Rev. Lett.* **65**, 1301; Suzuki, Y., 1993, *Proc. Theory and Phenomenology in Astroparticle and Underground Physics (TAUP '93)*, Gran Sasso, to be published.
[6] Bahcall, J.N., 1989, *Neutrino Astrophysics*, Cambridge, Cambridge Univ. Press.
[7] Mikheyev, S.P. and Smirnov, A. Yu., 1986, *Sov. J. Nucl. Phys.* **42**, 913.
[8] Wolfenstein, L., 1978, *Phys. Rev.* **D17**, 2369; 1979, *Phys. Rev.* **D20**, 2634.
[9] Abazov, A.I. *et al.*, 1991, Phys. Rev. Lett. **67**, 3332; Anosov, O.L. *et al.*, 1993, Nucl. Phys. **B31**, 111; Gavrin, V.N. *et al.*, 1992, *Proc. Intl. Conf. on High Energy Physics*, Dallas; Anosov, O.L. *et al.*, 1993, *Proc. Theory and Phenomenology in Astroparticle and Underground Physics (TAUP '93)*, Gran Sasso, to be published.
[10] Abdurashitov, J.N. *et al.*, 1994, Phys. Lett. **B**, to be published.
[11] Anselmann, P. *et al.*, 1992, Phys. Lett. **B285**, 376; Anselmann, P. *et al.*, 1994, Phys. Lett. **B**, to be published.
[12] Anselmann, P. *et al.*, 1992, Phys. Lett. **B285**, 390.
[13] Gelb, J.M. *et al.*, 1992, Phys. Rev. Lett. **69**, 1864; H. A. Bethe and J. N. Bahcall, 1991, Phys. Rev. D44. 2962.
[14] Chen, C.X. and Cherry, M.L., 1991, Ap. J. Lett. **377**, L105; S.A. Bludman *et al.*, 1993, Phys. Rev. D **47**, 2220; L. Krauss *et al.*, 1993, Phys. Lett. B **299**, 94; P.I. Krastev and S.T. Petcov, 1993, Phys. Lett. B **299**, 99.
[15] Raghavan, R.S. *et al.*, 1991, Phys. Rev. D **44**, 3786.
[16] McDonald, A.B., 1992, *Proc. Franklin Symp. on Discovery of the Neutrino*, Philadelphia.

Figure Captions:

Fig. 1. Proton-proton reaction chain, expected neutrino energies, and predicted fluxes.

Fig. 2. Data for the 1990, 1991, and 1992 runs shown as a function of the mean ^{71}Ge lifetime. The energy spectra during the first two mean lifetimes are shown on the left, the normalized spectra for the time periods ≥3 mean lifetimes on the right. The shaded areas indicate the expected ^{71}Ge K peak position.

Fig. 3. Count rate summed over 16 solar neutrino runs (1990-92) as a function of elapsed time since extraction. The dashed line shows the expected distribution for a 16.49 day mean lifetime.

Fig. 4. Distribution of derived SNU values for the 16 individual sets (solid histogram) compared to the result of a Monte Carlo simulation assuming an average value of 70 SNU (dashed histogram).

Fig. 5. Best fit values and 2 sigma uncertainties for each of the individual data runs. The combined best fit value and 1 sigma uncertainty is shown as the diamond on the right.

Fig. 6. SAGE proportional counters.

Fig. 7. Measured Kamiokande II recoil electron angular distribution after 1040 live detector days (from Hirata et al.[5]). Figure shows the cosine of the angle between the electron direction and the sun, and clearly shows an isotropic background plus an excess from the direction of the sun. The solid histogram shows the expected distribution based on a Monte Carlo simulation.

Fig. 8. Kamiokande II electron energy distribution for events with $\cos\theta_\odot > 0.9$. The solid histogram is the result of a Monte Carlo simulation using the known ν_e elastic cross section, the known shape of the ^{8}B neutrino spectrum, the detector energy resolution, and the flux predicted by Bahcall and Ulrich. The dashed histogram gives the expected result scaled down by 0.46.

Fig. 9. The regions in neutrino mass difference vs. mixing angle space allowed by the experimental results (from Chen and Cherry[14]). The shaded region is the area permitted (with 95% confidence) by Kamiokande II; the cross-hatched area is that permitted by Homestake. Both regions contract and the intersection region decreases at the 68% confidence level. The solid lines correspond to gallium counting rates of 10 - 120 SNU.

Fig. 10. Regions in δm^2 - mixing angle space allowed by Homestake, Kamiokande II, and gallium (from Anselmann et al.[12]). Six representative possible MSW solutions are labelled.

Fig. 11. Expected recoil electron spectra to be measured by SuperKamiokande for the MSW solutions shown in Fig. 10. Statistical errors are shown for both SuperKamiokande and Kamiokande II.

Fig. 12. Schematic representation of the SuperKamiokande detector.

Fig. 13. SuperKamiokande anticounter.

The *pp* Reaction Chains

*pp*I	*pp*II	*pp*III
$p + p \rightarrow d + e^+ + \nu_e$		
or $p + e^- + p \rightarrow d + \nu_e$		
$d + p \rightarrow {}^3He + \gamma$		
${}^3He + {}^3He \rightarrow {}^4He + p + p$ -or-	${}^3He + {}^4He \rightarrow {}^7Be + \gamma$	
	${}^7Be + e^- \rightarrow {}^7Li + \nu_e$ -or-	${}^7Be + p \rightarrow {}^8B + \gamma$
	${}^7Li + p \rightarrow {}^4He + {}^4He$	${}^8B \rightarrow {}^8Be^* + e^+ + \nu_e$
		${}^8Be^* \rightarrow {}^4He + {}^4He$

Main Neutrino Producing Reactions in the Sun, Maximum Neutrino Energy, and the Integrated Flux Predicted by the Standard Solar Model

Solar Reaction	Max. Neutrino Energy (MeV)	Predicted Total Flux ($cm^{-2}sec^{-1}$)	Neutrino Capture Rate (SNU) ${}^{37}Cl(\nu,e){}^{37}Ar$	${}^{71}Ga(\nu,e){}^{71}Ge$
$p + p \rightarrow d + e^+ + \nu_e$	0.42	6.1×10^{10}	0	70.8
$p + e^- + p \rightarrow d + \nu_e$	1.44	1.5×10^8	0.2	3.0
$e^- + {}^7Be \rightarrow {}^7Li + \nu_e$	0.86	4.0×10^9	1.1	34.3
${}^8B \rightarrow {}^8Be + e^+ + \nu_e$	14.10	5.6×10^6	6.1	14.0
${}^{13}N \rightarrow {}^{13}C + e^+ + \nu_e$	1.15	5×10^8	0.1	3.8
${}^{15}O \rightarrow {}^{15}N + e^+ + \nu_e$	1.73	4×10^8	0.3	6.1
			7.9	132.0

Figure 1

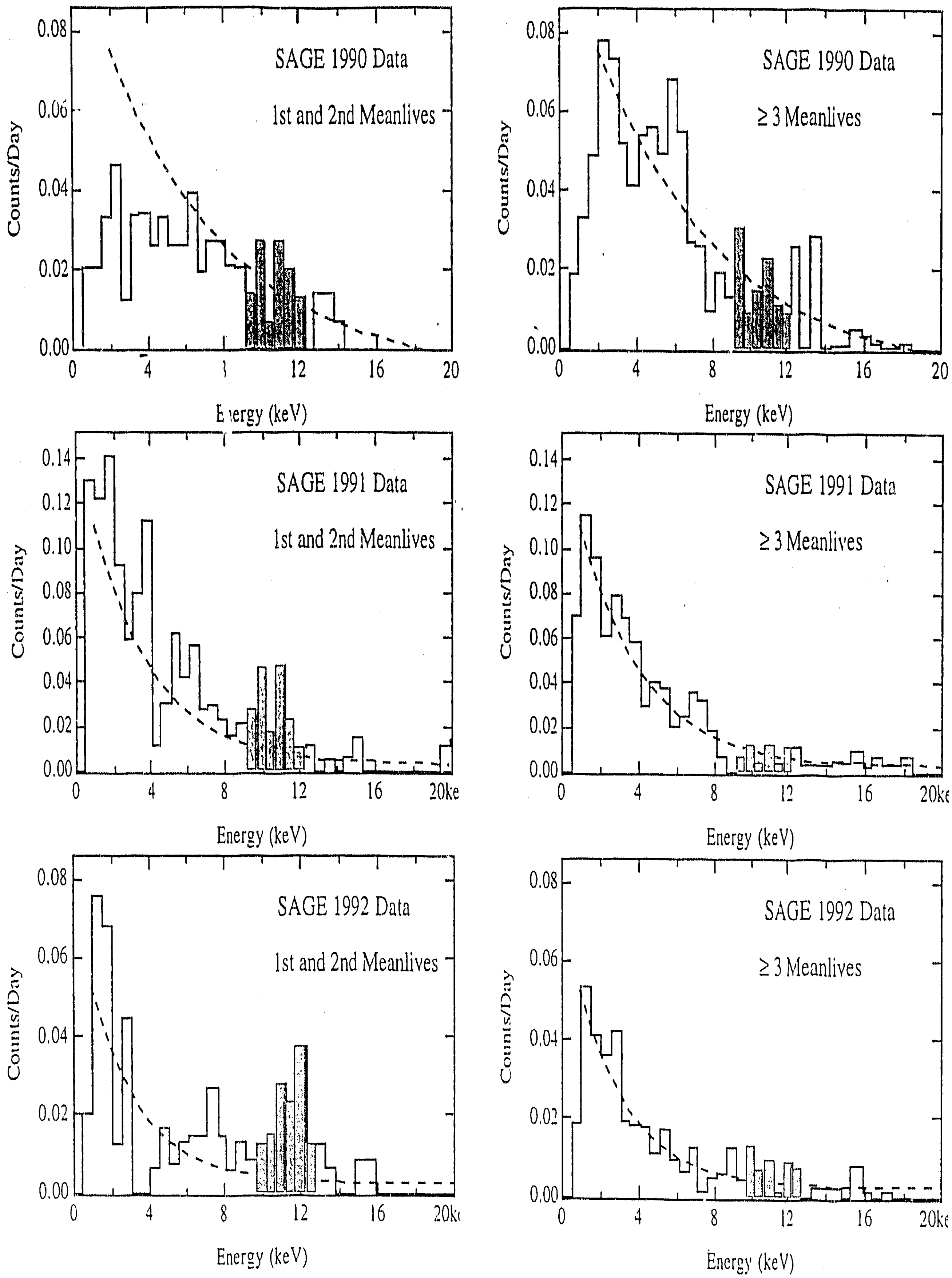
SAGE 1990 Data
1st and 2nd Meanlives
≥ 3 Meanlives
SAGE 1991 Data
1st and 2nd Meanlives
≥ 3 Meanlives
SAGE 1992 Data
1st and 2nd Meanlives
≥ 3 Meanlives
Counts/Day
Energy (keV)

Figure 2

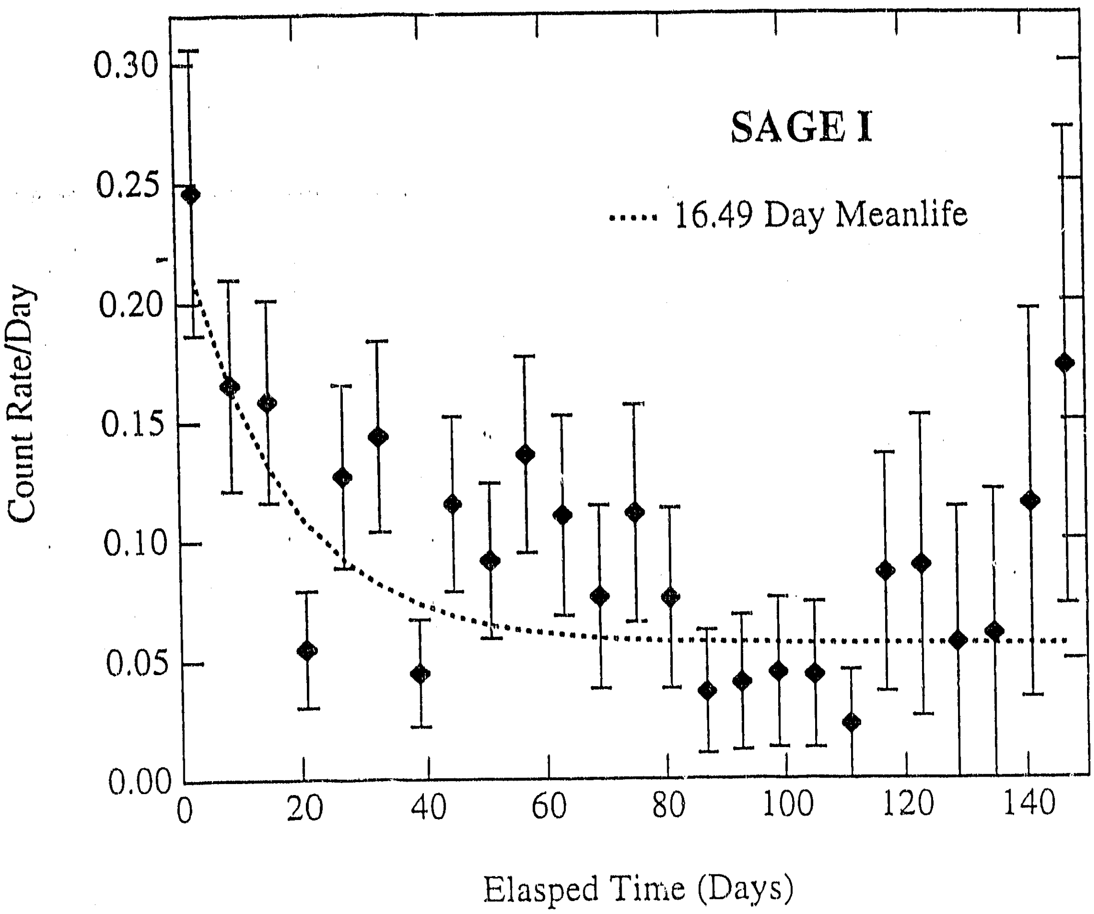
SAGE I
16.49 Day Meanlife
Count Rate/Day
0.30
0.25
0.20
0.15
0.10
0.05
0.00
0
20
40
60
80
100
120
140
Elasped Time (Days)

Figure 3

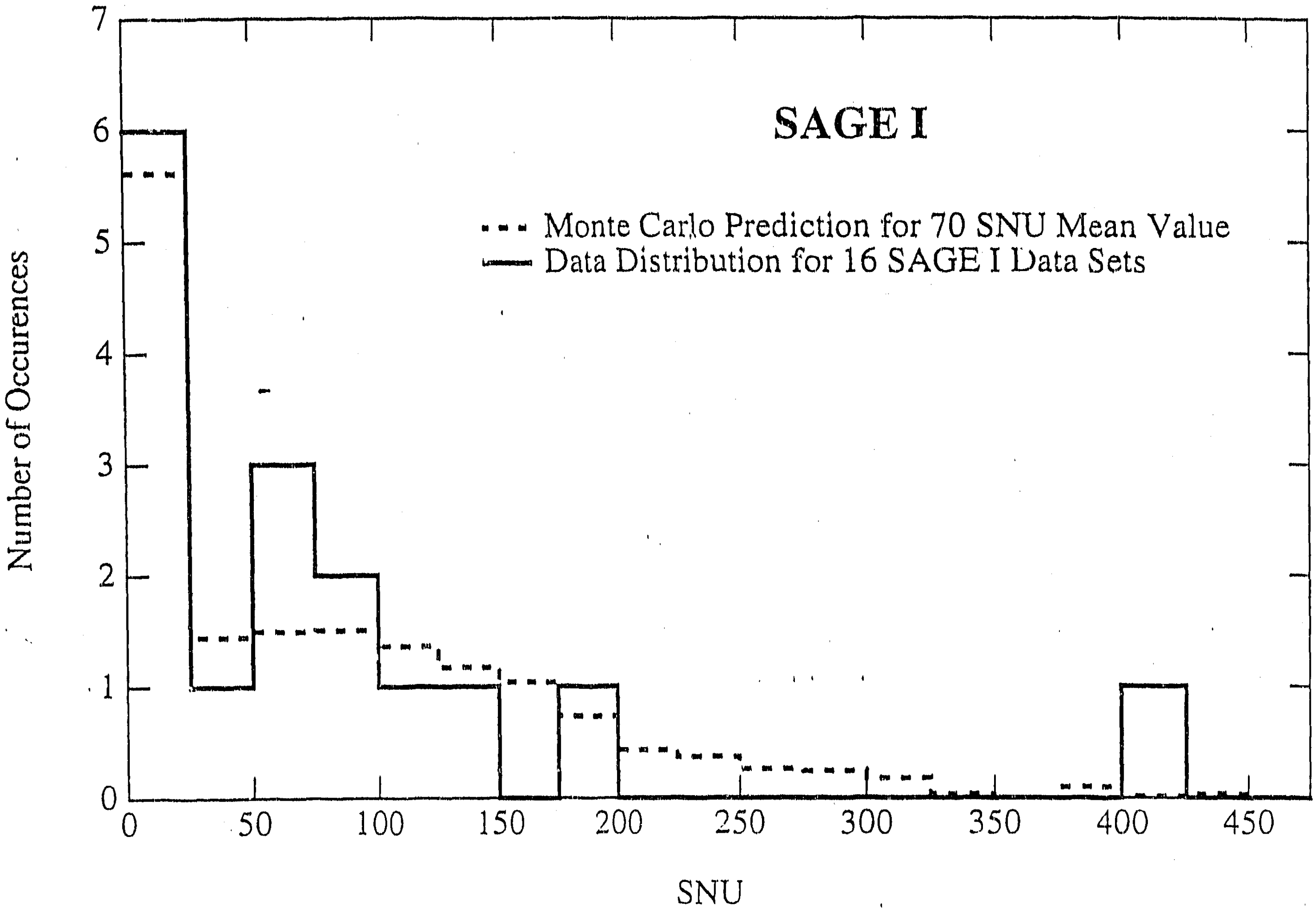
SAGE I
Monte Carlo Prediction for 70 SNU Mean Value
Data Distribution for 16 SAGE I Data Sets
Number of Occurences
0
1
2
3
4
5
6
7
0
50
100
150
200
250
300
350
400
450
SNU

Figure 4

PRELIMINARY SAGE I RESULTS

70 ± 19 (stat.) ± 10 (sys.) SNU   (.53 SSM)

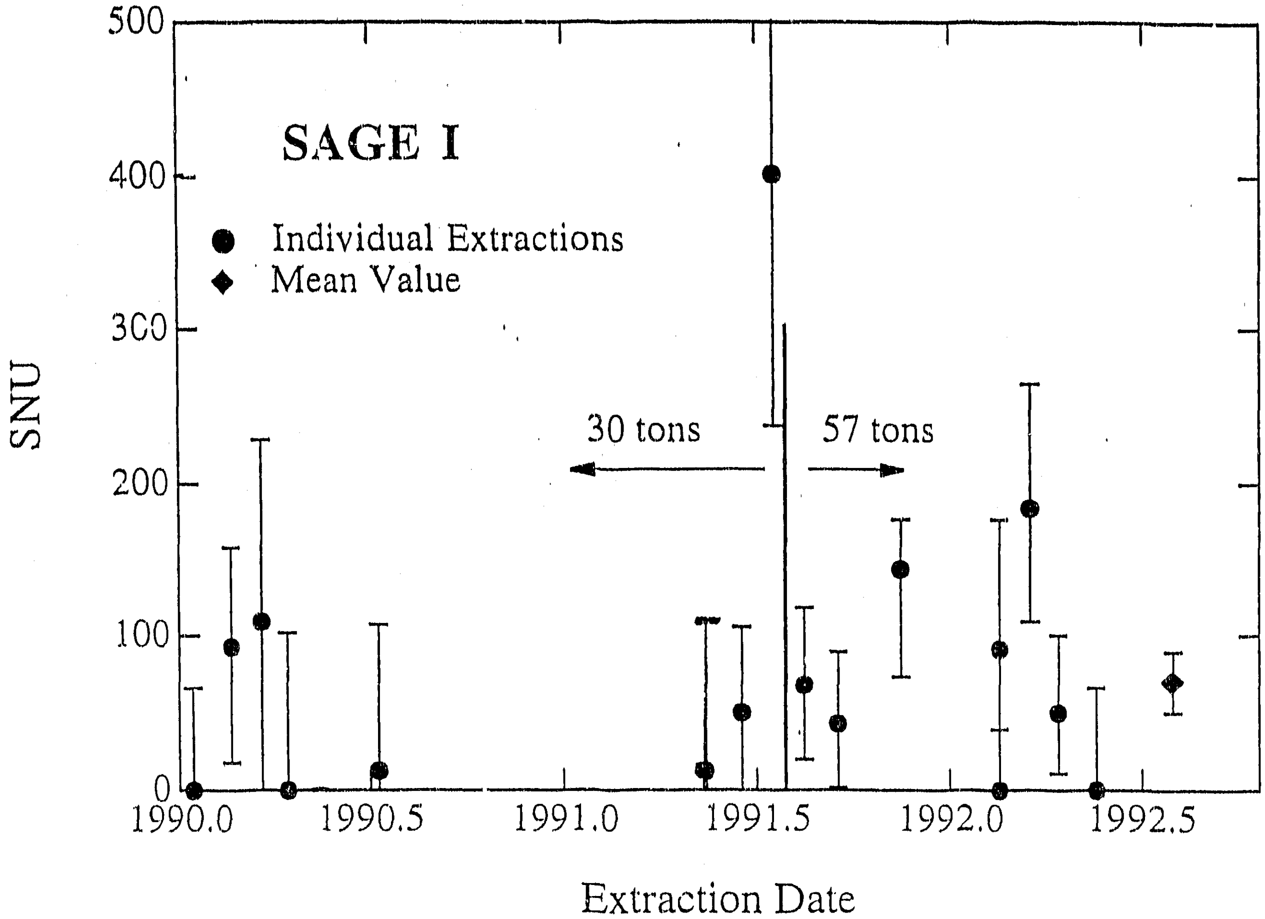

Systematics

Efficiencies	5 SNU
Rise time	7 SNU
Backgrounds	3 SNU
Radon	5 SNU

Figure 5

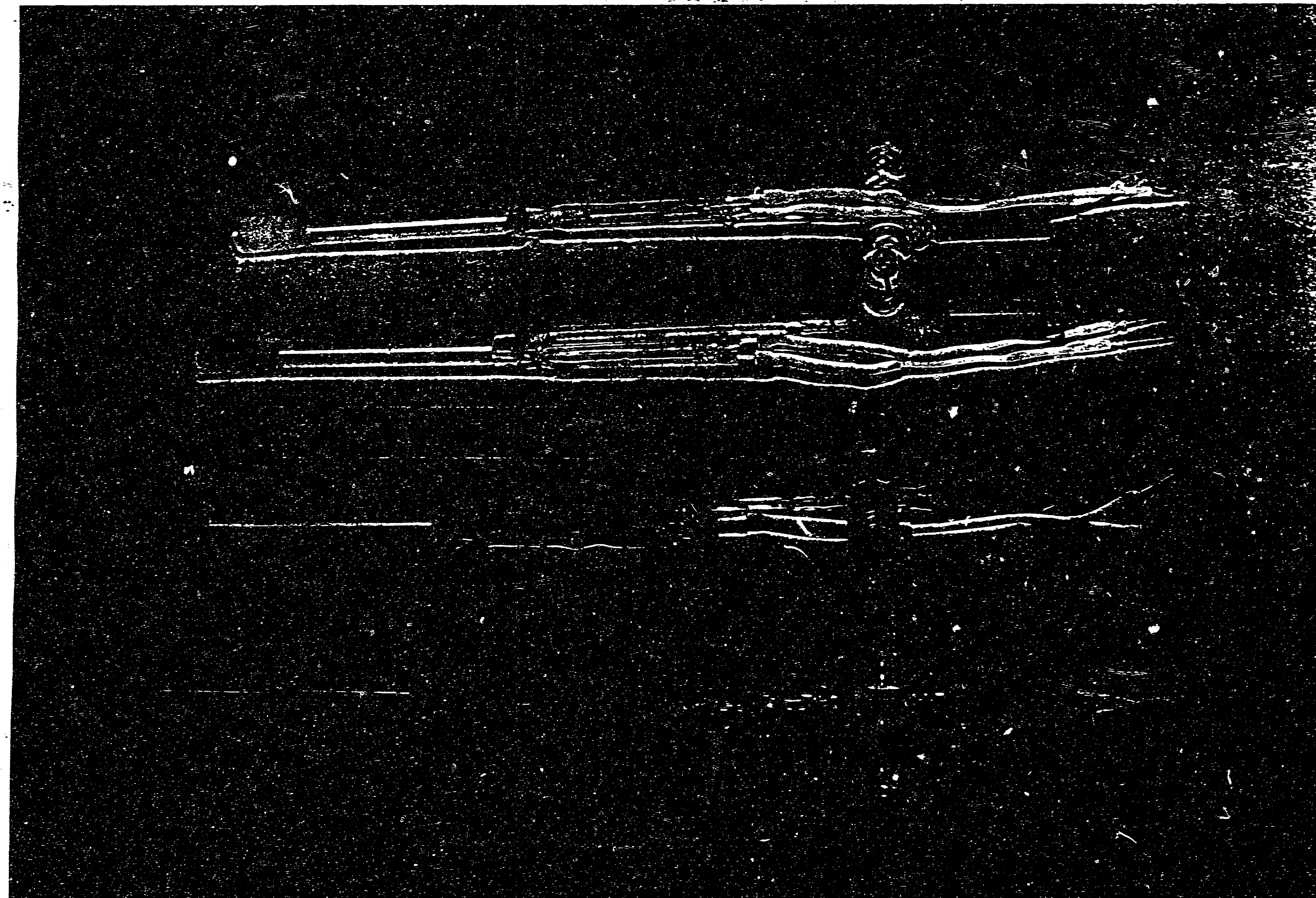

Figure 6

KAM-II (1040day) + KAM-III (395day)

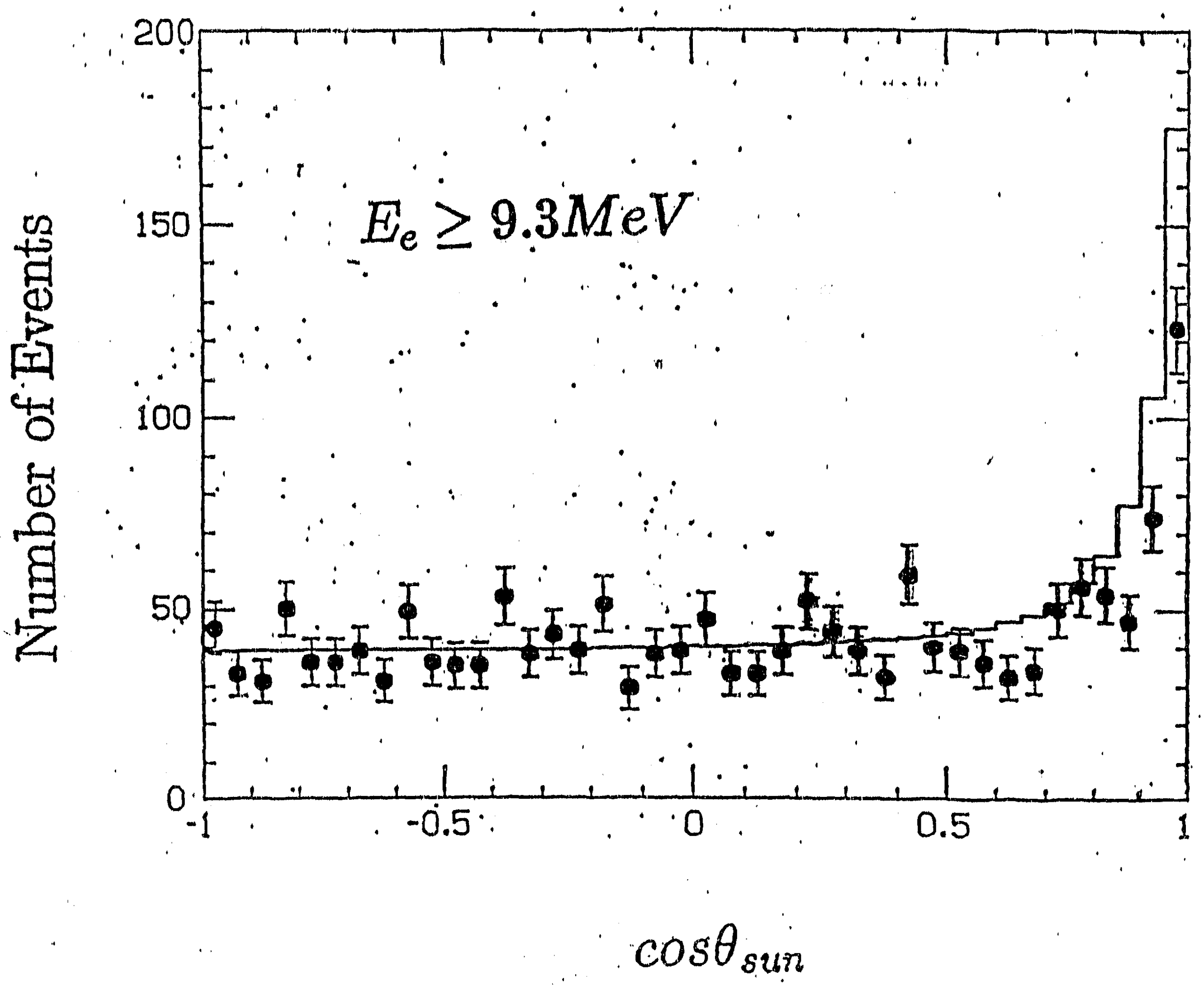

$$\mathrm{KAM-II} \quad 0.46 \pm 0.05(\mathrm{stat.}) \pm 0.06(\mathrm{syst.})$$

$$\mathrm{KAM-III} \quad 0.55 \pm 0.07(\mathrm{stat.}) \pm 0.06(\mathrm{syst.})$$

$$\mathrm{KAM-II+III} \quad 0.49 \pm 0.04(\mathrm{stat.}) \pm 0.06(\mathrm{syst.})$$

Figure 7

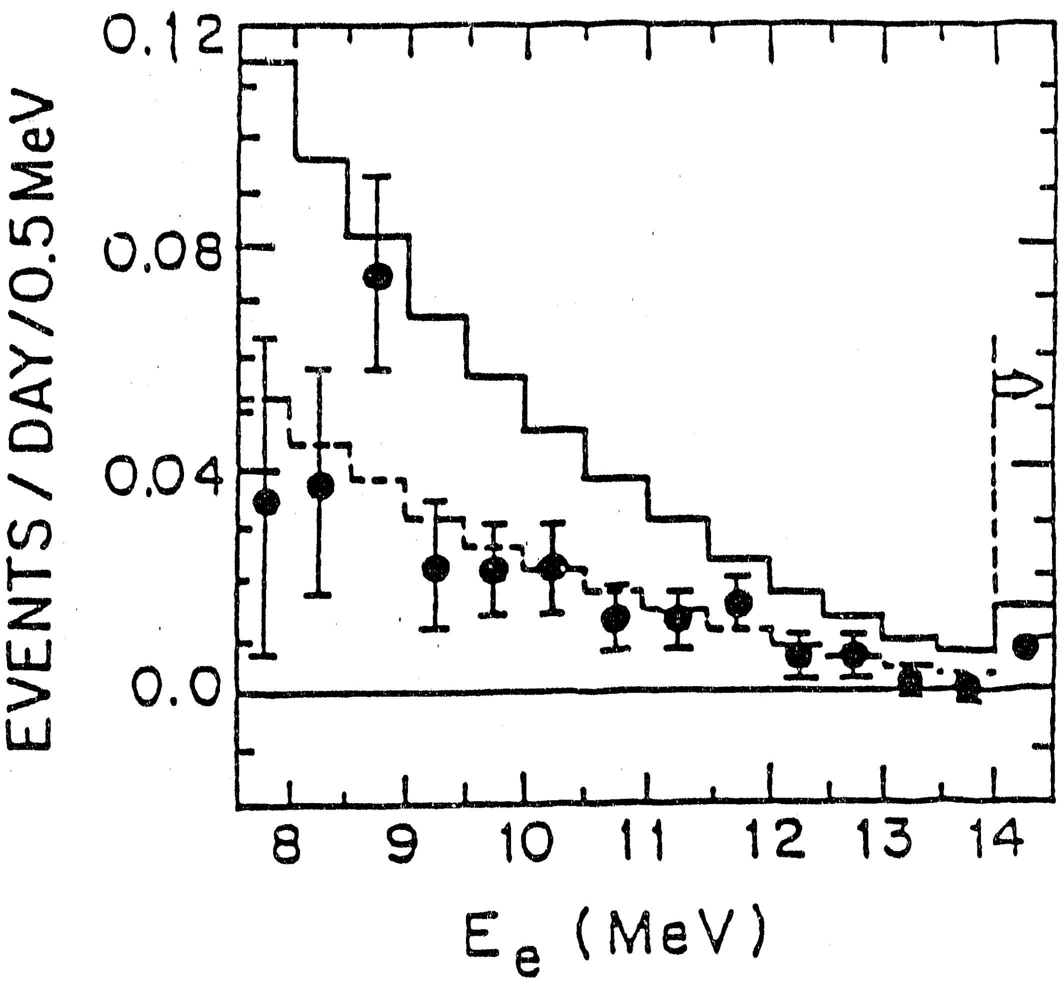

Figure 8

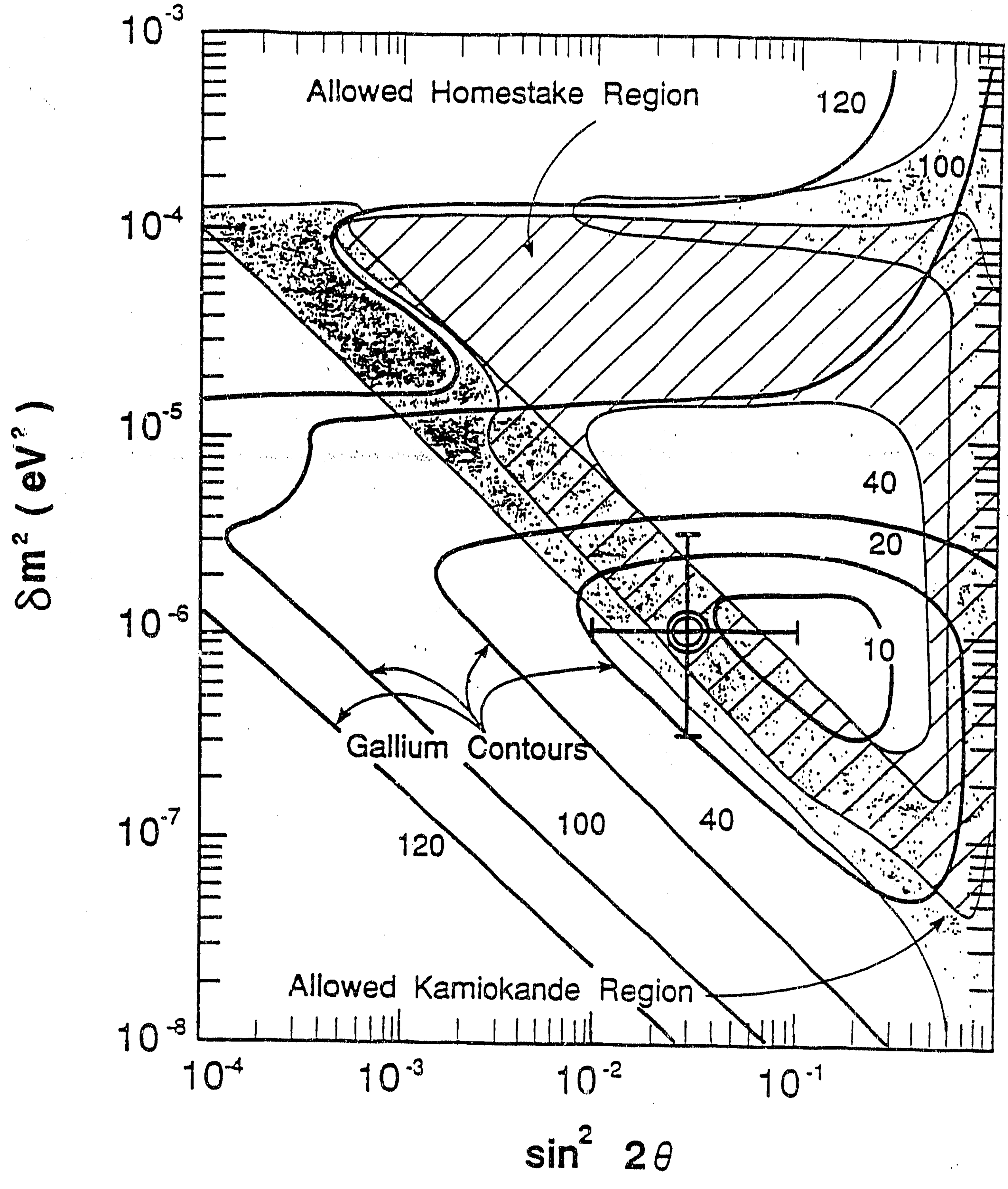
Allowed Homestake Region
120
100
40
20
10
Gallium Contours
120
100
40
Allowed Kamiokande Region
10^-3
10^-4
10^-5
10^-6
10^-7
10^-8
δm² (eV²)
10^-4
10^-3
10^-2
10^-1
sin² 2θ

Figure 9

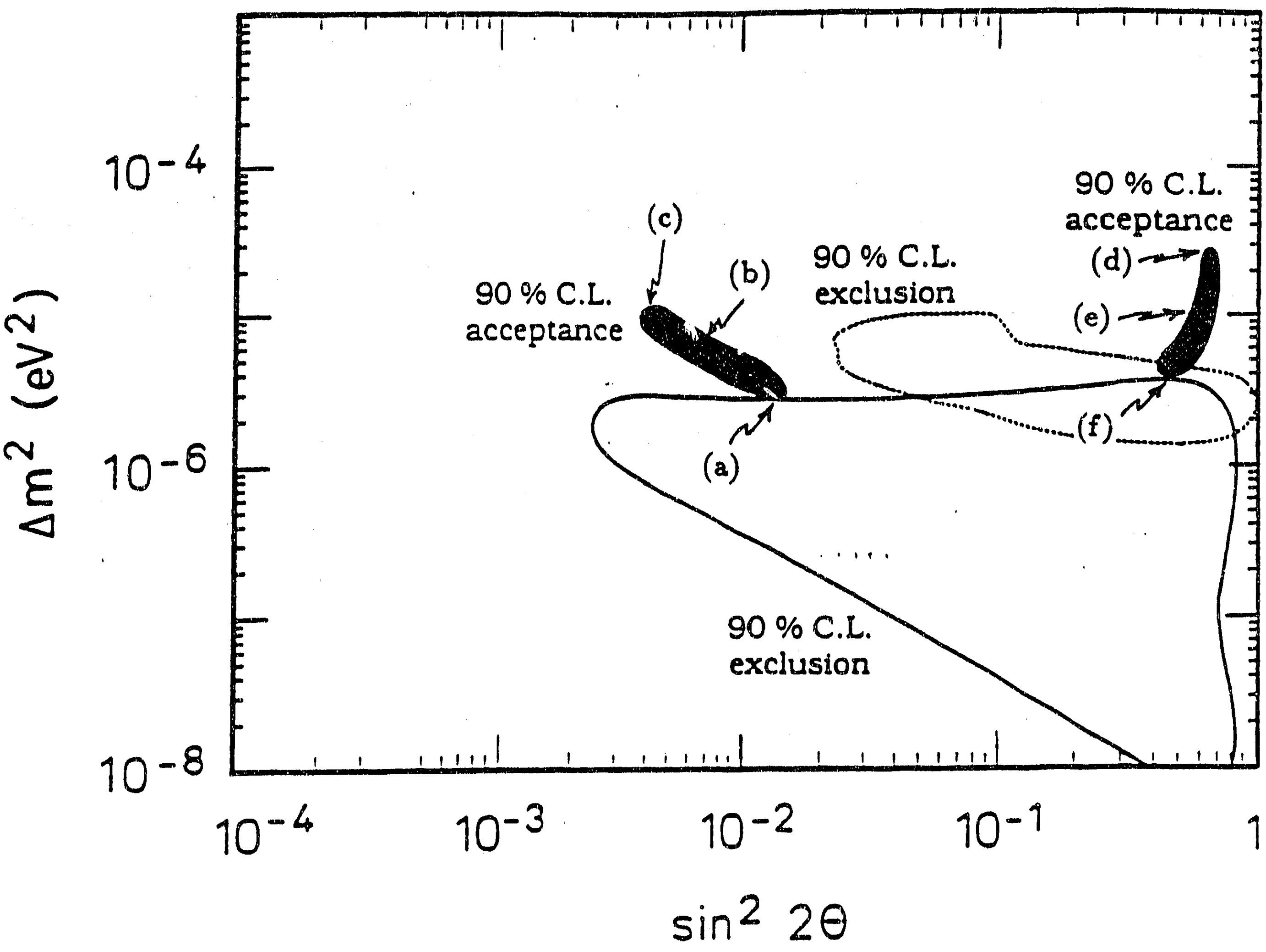

90 % C.L.
acceptance
(d)
(e)
(f)
(c)
(b)
90 % C.L.
acceptance
90 % C.L.
exclusion
(a)
90 % C.L.
exclusion
10^{-4}
10^{-6}
10^{-8}
Δm^2 (eV^2)
10^{-4}
10^{-3}
10^{-2}
10^{-1}
1
$\sin^2 2\Theta$

Figure 10

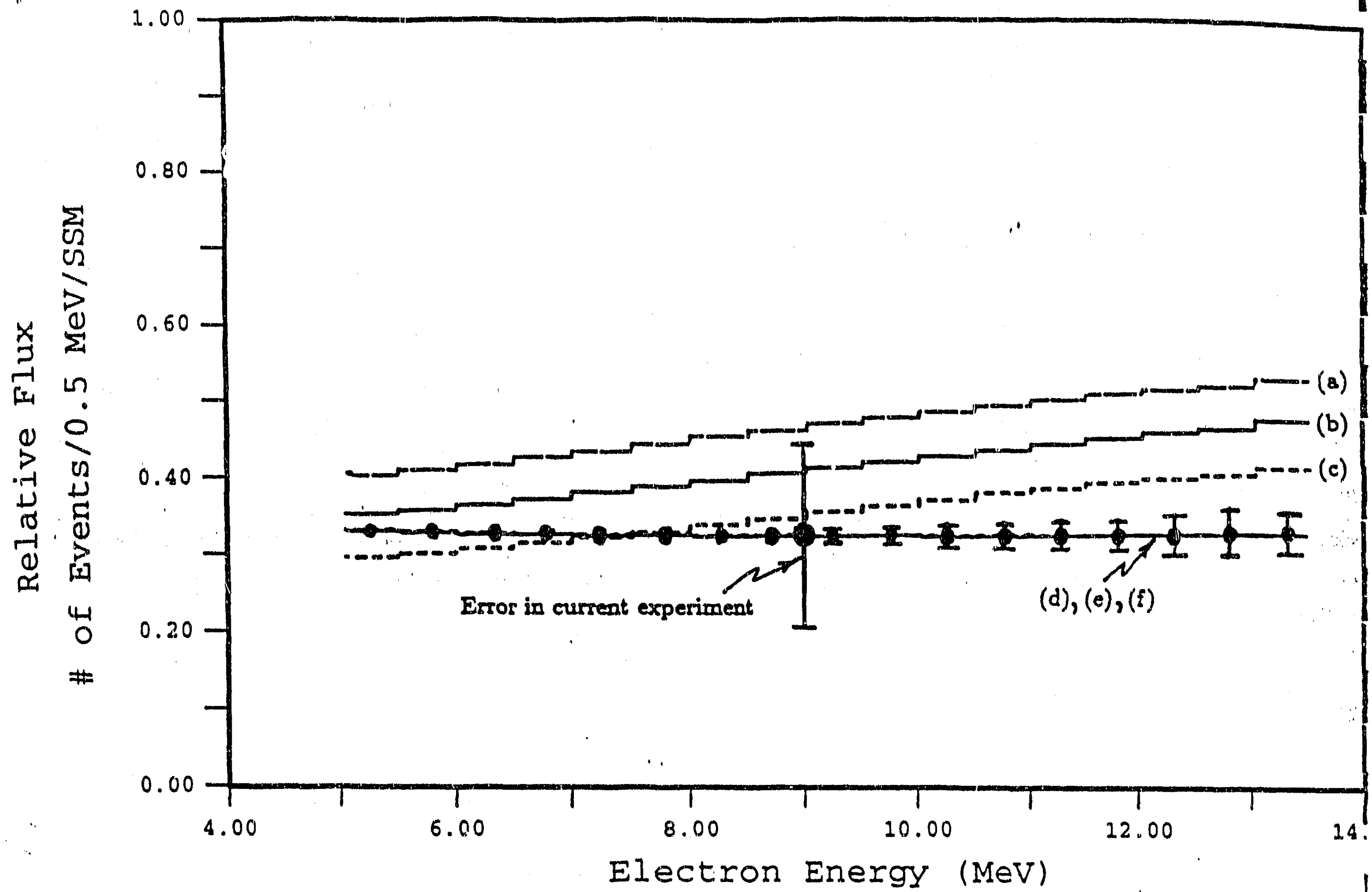

Relative Flux
# of Events/0.5 MeV/SSM
1.00
0.80
0.60
0.40
0.20
0.00
4.00
6.00
8.00
10.00
12.00
14.
Electron Energy (MeV)
(a)
(b)
(c)
Error in current experiment
(d), (e), (f)

Figure 11

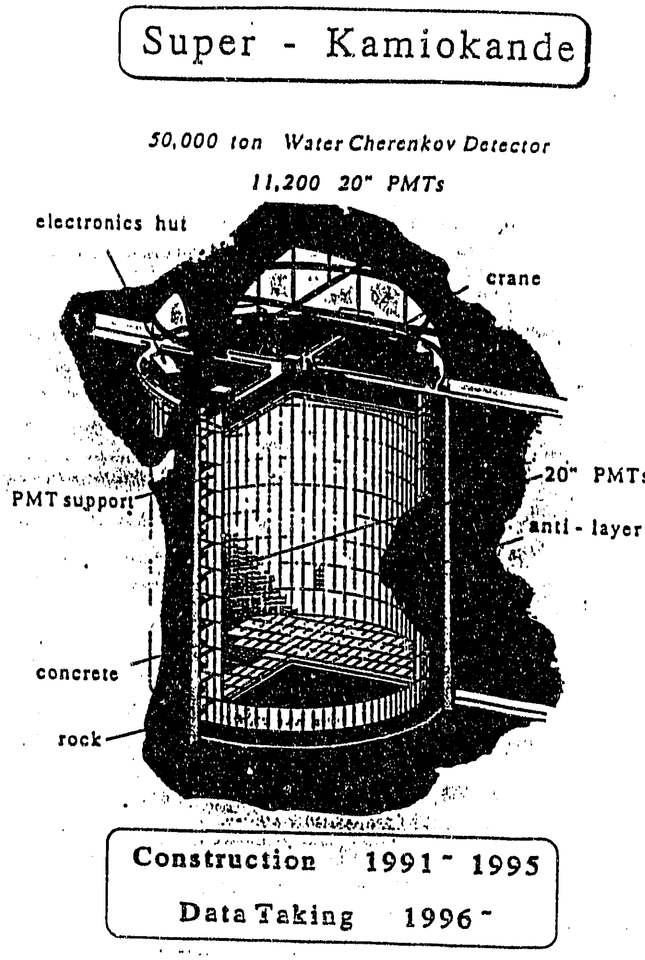

Figure 12a

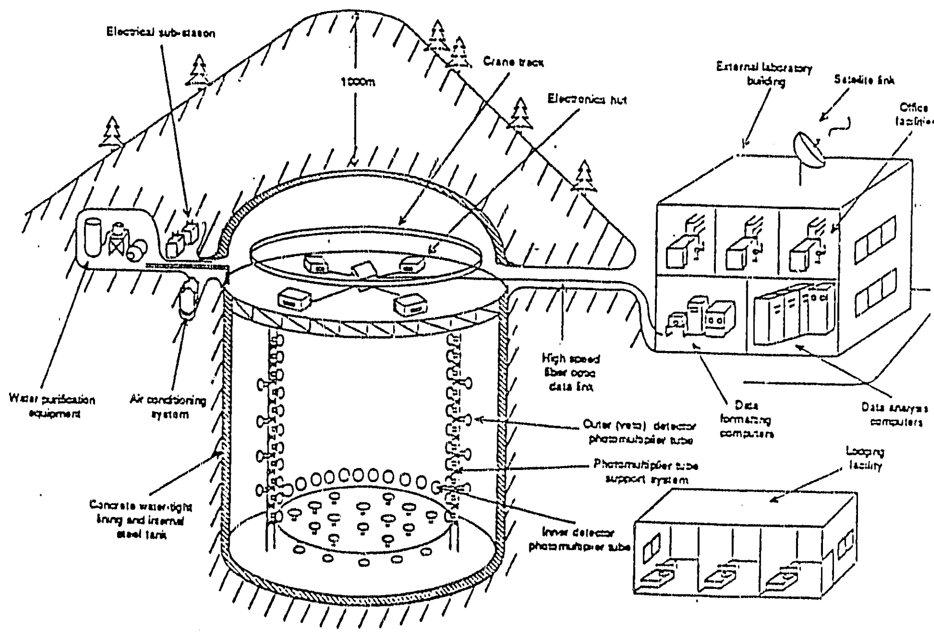

Figure 12b

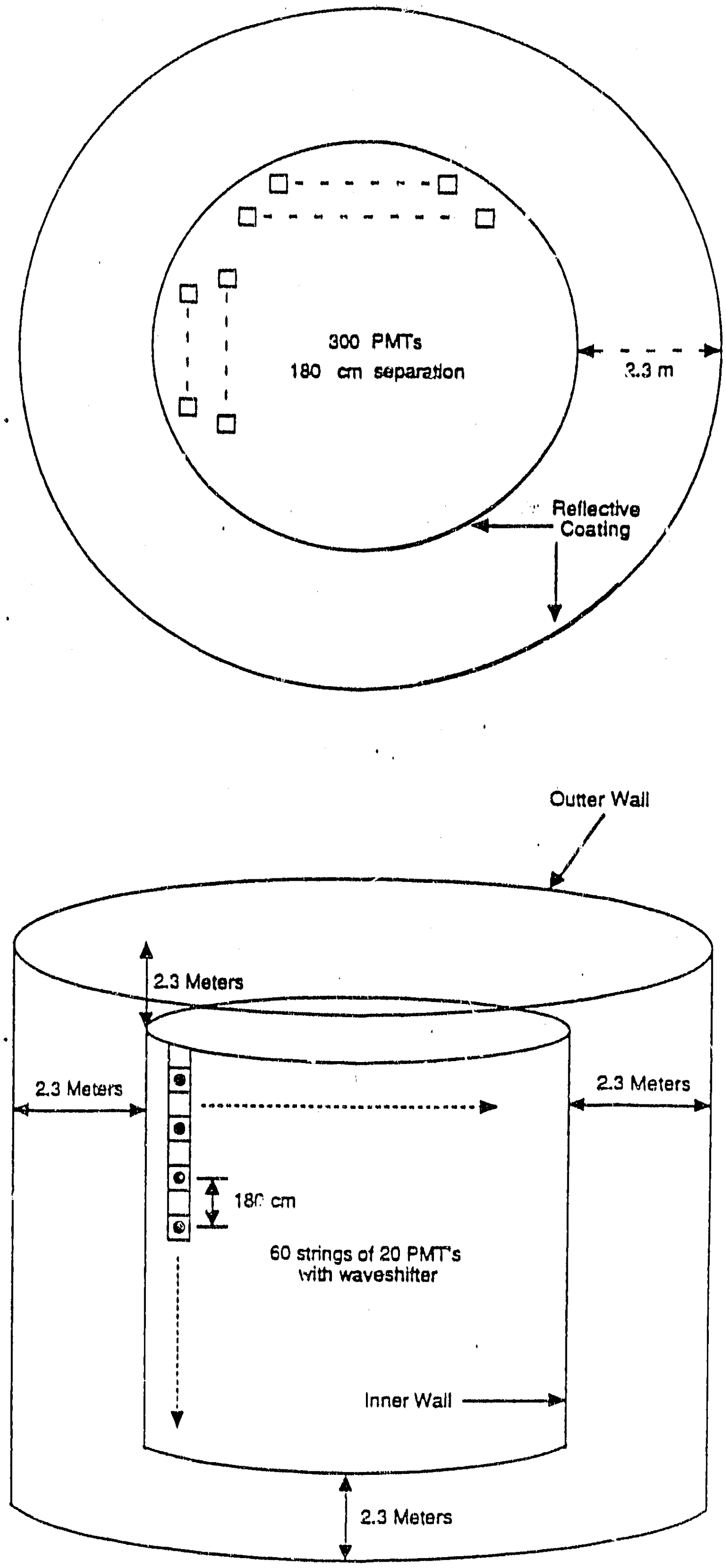
300 PMTs
180 cm separation
2.3 m
Reflective
Coating
Outter Wall
2.3 Meters
2.3 Meters
2.3 Meters
180 cm
60 strings of 20 PMT's
with waveshifter
Inner Wall
2.3 Meters

Figure 13

AIIM

Association for Information and Image Management

1100 Wayne Avenue, Suite 1100
Silver Spring, Maryland 20910

301/587-8202

Centimeter

Inches

MANUFACTURED TO AIIM STANDARDS
BY APPLIED IMAGE, INC.

DATE

FILMED

5/25/95

END